#### Research Article

Xiaolong Sun, Zhengbing Yuan, Zhenying Huang, Qin Xu, Yongqiang Zhu, Xinquan Xu, Junshen Yuan, Zhisheng Liu, Yikang Zhang, Qian Chen, and Alex Hay-Man Ng\*

# Applying solution of spray polyurea elastomer in asphalt binder: Feasibility analysis and DSR study based on the MSCR and LAS tests

https://doi.org/10.1515/ntrev-2022-0508 received August 3, 2022; accepted January 2, 2023

Abstract: The polyurea elastomer (PUA) powder modifier was prepared by the method of spraying-initial crushing-fine grinding, and then, the PUA-modified asphalt was produced. The typical functional structure of PUA was identified and characterized. The apparent viscosity of PUA-modified asphalt was tested at different temperatures. The impact of particle size and content of PUA on creep and recovery properties of asphalt at high temperature was investigated through the multiple stress creep recovery test. The mesothermal fatigue behavior of PUAmodified asphalt was evaluated by means of time sweep and linear amplitude sweep. Results indicated that the high elastic properties of PUA materials might depend on the spherical structure inside PUA material. The diameter of functional structure was around 20 µm and presented as 3D ball structure. The increase in PUA particle size would lead to the increase in cracks and folds in the bonding surface PUA modifier could improve by about 50% of the apparent viscosity significantly. Furthermore, PUA modifier could promote the high-temperature rutting resistance and middle-temperature fatigue property of asphalt. The improving effect on R could reach almost 28% and the 0.075 mm could be the best application size of PUA.

**Keywords:** PUA, rheological properties, microstructure, asphalt binder

## 1 Introduction

Asphalt pavement has been widely used in road pavement because of its good mechanical properties, smoothness, and road comfort. However, subjected to extreme weather and heavy traffic conditions, rutting, spalling, and cracking is prone to emerge in asphalt pavement during the service period [1,2], which leads to negative effect on its road performance and durability. To mitigate the failure of asphalt pavement, researchers home and abroad have carried out some research on the modification technology of road materials, expecting upgrading the durability of asphalt pavement during its service life. In recent years, polymer modifier as a high-performance modifier has become a research hot spot in the field of asphalt modification gradually.

Among existing polymer modifiers, the block copolymer has excellent aging resistance, oil resistance, and adhesion, which possesses great potential in asphalt modification [3,4]. Block copolymers are mainly composed of soft segment diol, hard segment diisocyanate, and diffusion chain. The soft segment has high elastic state, low modulus, and good flexibility at room temperature, while the hard segment has glass state, high modulus, and high strength. The combined structure of hard and soft segments promotes the flexibility and rigidity of block copolymers. In the modification process, the complex intermolecular force could be achieved between block copolymer and asphalt, which promotes the formation of complex multiphase system in the modified asphalt, so as

Zhengbing Yuan: Shanxi Transportation Holdings Group Co., Ltd., Taiyuan 030006, China

Zhenying Huang, Qin Xu: Guangzhou HuaHui Traffic Technology Co., Ltd., Guangzhou 510335, China

Yongqiang Zhu: Guangdong GuanYue Highway & Bridge Co., Ltd., Guangzhou 511450, China

Xinquan Xu: Guangdong HuaLu Transport Technology Co., Ltd., Guangzhou 510420, China

Zhisheng Liu: Shanxi Transportation Holdings Group Co., Ltd., Taiyuan 030006, China; The Key Laboratory of Road and Traffic Engineering, Ministry of Education, Tongji University, Shanghai 201804, China Qian Chen: Key Laboratory of Road Structure & Material of Transport Ministry, Chang'an University, Xi'an 710064, China

<sup>\*</sup> Corresponding author: Alex Hay-Man Ng, School of Civil and Transportation Engineering, Guangdong University of Technology, Guangzhou 510006, China, e-mail: hayman.ng@gdut.edu.cn Xiaolong Sun, Junshen Yuan, Yikang Zhang: School of Civil and Transportation Engineering, Guangdong University of Technology, Guangzhou 510006, China

to implement the property optimization of asphalt materials [5-7]. Domestic and foreign scholars have carried out relevant studies on block copolymer to clarify its modifying effect on asphalt. Behravan et al. [8], Jomaa et al. [9], and Xu [10] noticed that polyurethane materials could improve the deformation resistance, high temperature resistance, and aging resistance of asphalt materials. Through a series of property tests, Sun [11] found that polyurethane material has the ability to improve the low-temperature crack resistance of asphalt binder. Peng [12] concluded that polyurethane materials could maintain the tensile strength of asphalt and improved the peel resistance of asphalt binder through pull-off test and ultrasonic washing test. Current research [13-16] showed that, different from commonly used modifiers such as styrenebutadiene-styrene block copolymer, styrene-butadiene rubber, polyethylene, and ethylene-vinyl acetate copolymer, polyurethane block copolymer has better compatibility with asphalt and could react with some internal components of asphalt to achieve the chemical modification of asphalt materials, so as to solve the problems of layering and segregation of modifiers in asphalt. Regarding achieving performance optimization, Jin [17], Liu et al. [18], Gao et al. [19], and Cong et al. [20] also noticed that polyurethane block copolymer could endow asphalt with self-healing performance, and asphalt pavement cracks could be self-healed to a certain extent when suffering from the impact of external environment.

Currently, block copolymer-modified asphalt was prepared normally by adding different components of block copolymer into asphalt and mixing them by shear stirring. This method could achieve excellent mixing between asphalt and block copolymer; however, the compatibility, dispersion, and swelling between block copolymer and asphalt might lead to negative effect on the combined structure formation of soft segment diol and hard segment diisocyanate inside asphalt [21–23]. Therefore, in view of such problem, it has become a new research topic whether the viscoelastic modification effect on asphalt could be achieved by using fine grinding the cured block copolymer to prepare modified asphalt materials.

For exploring the applying feasibility of fine-grinded block copolymer in asphalt binder, the polyurea elastomer

(PUA) precursor copolymer was selected as the modifying object, and the PUA material was produced into powder materials of different particle sizes by the spraying-grinding-fine grinding method, and the modified asphalt was prepared. To explore the existing form of PUA in asphalt, the particle size and microstructure of PUA particle material (4-5 mm) and PUA powder (0.075, 0.15, and 0.3 mm) were identified and analyzed by laser confocal scanning microscope (LCSM) and laser particle size analyzer (LPSA). Based on the scanning electron microscope (SEM) test, the dispersion characteristics of PUA modifier in asphalt and the microscopic interface between PUA and asphalt were observed. The apparent viscosity of PUA-modified asphalt and matrix asphalt was compared at different temperatures. According to the multiple stress creep recovery (MSCR) test, the influence of particle size and content of PUA material on the high temperature creep performance of asphalt was analyzed. Based on the time sweep test and linear amplitude sweep (LAS) test, the variation in mesothermal fatigue performance of PUA-modified asphalt was investigated, which provided a new solution for the application of block copolymer in asphalt pavement materials.

## 2 Materials and methodology

#### 2.1 Materials

#### 2.1.1 PUA material

The PUA material contains acrylic functional groups and urethane bonds, whose cured adhesive has high wear resistance, adhesion, flexibility, high peel strength, excellent low-temperature resistance, and weather resistance. The technical properties of PUA are presented in Table 1.

#### 2.1.2 Asphalt

To clarify the modification effect of PUA material on asphalt precisely, 70# asphalt was selected as the matrix asphalt. The penetration at 25°C was 4.33 mm, the ductility at 10°C was 10.3 cm, and the softening point was 46°C.

Table 1: Technical properties of PUA

PUA type	Solid content (%)	Viscosity (cps)	Tensile strength (MPa)	Elongation at break (%)
PUA-100	81-85	≤800	28	375
Test standard	ASTM D2369	ASTM D4287	ASTM D638	ASTM D638

All technical indices of matrix asphalt met the relevant performance requirements.

# 2.1.3 Preparation of PUA modifier and PUA-modified asphalt

To clarify the functional mechanism of PUA materials, PUA particles were prepared as the basic material for subsequent material grinding treatment. To achieve the modifying effect of PUA material on asphalt carrier, this research hoped to grind the PUA particles  $(4~\text{mm}\times4~\text{mm}\times2~\text{mm})$  into the powder of the fineness between 100 and 200 mesh. However, it was found in the preliminary grinding process that due to the good elasticity of the PUA material, the effect of grinding ball would be completely absorbed by the PUA particles and PUA powder was failed to obtain. Regarding this, the liquid nitrogen cooling cryogenic grinding method was adopted to grind PUA materials. The low-temperature grinding method of PUA material is mainly as follows (detailed in Figure 1):

1) First, the proper amount of PUA raw materials was placed into the hopper of preparing equipment. The H2O/35PUA high-pressure spraying machine was used to prepare PUA film specimens and the technical

- parameters was adjusted. The thickness of the molded specimens needed to be measured and any five points of specimen must be within the range of  $2 \pm 0.1$  mm.
- 2) The 2 mm thick PUA film sample was cut into particles with the side length of 4–5 mm through using paper cutter. In the cutting process, the cutting parameters were set accurately to ensure that the cutting surface was neat and smooth.
- 3) The PUA particles was put into the storage bin of the grinding equipment, and the storage bin was frozen by liquid nitrogen. Meanwhile, then, the PUA particles and liquid nitrogen were mixed through a stirring device to confirm the fully contact between PUA and liquid nitrogen.
- 4) When cooled to the glass transition temperature, the PUA particles were sent to the grinder through the raw material conveyor for crushing. The crushed powder materials were sent to the secondary cyclone collector and then were discharged out of the machine through the electric discharge air lock valve.
- 5) The prepared PUA materials were sieved into PUA powder of 0.075, 0.15, and 0.3 mm. The dosage of 0.075 mm PUA material was 3, 6, and 9% by the matrix asphalt mass, and 0.15 mm PUA and 0.3 mm PUA were 6% by that. The mixture ratio of modifiers was named as

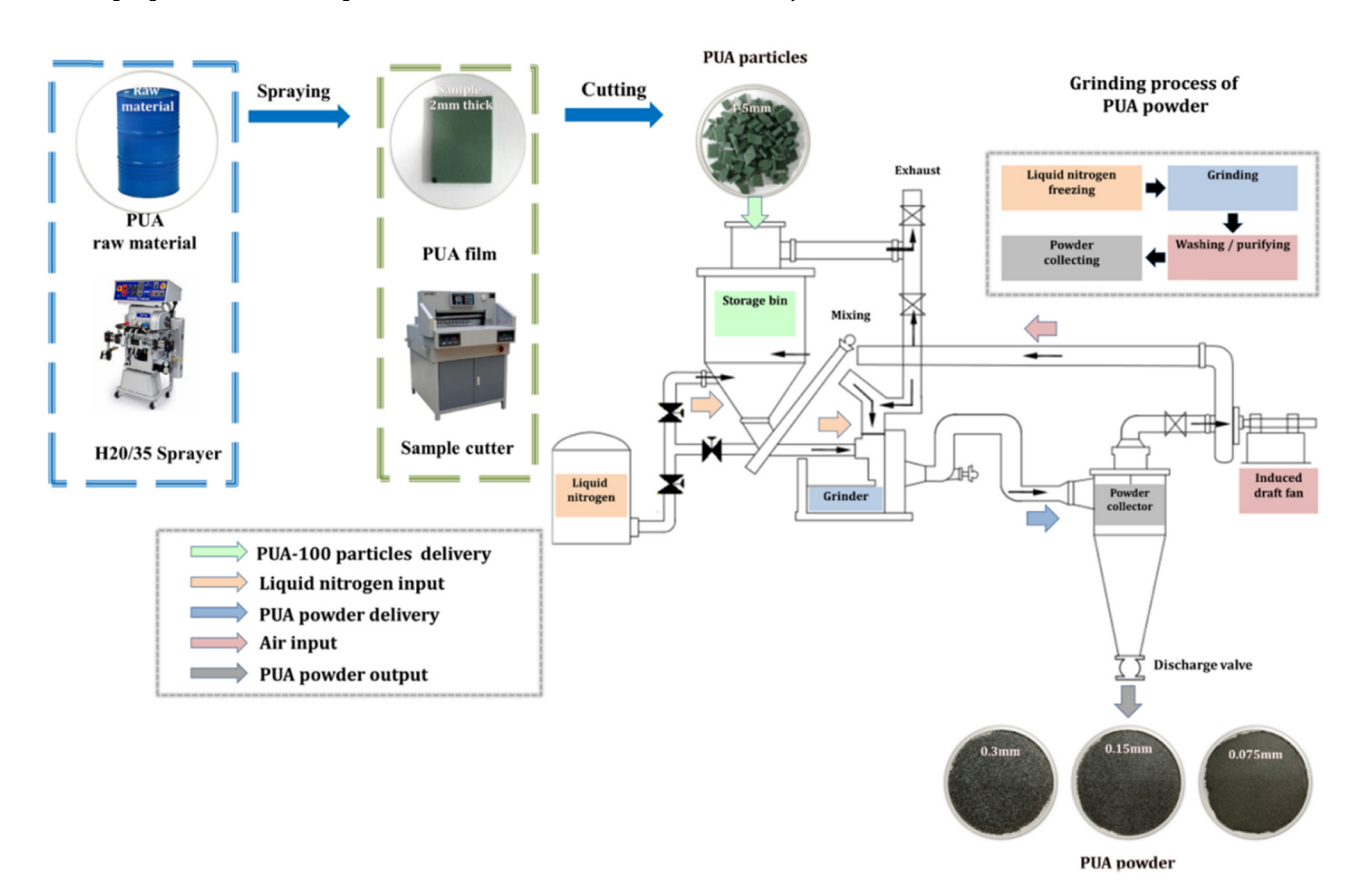


Figure 1: PUA asphalt preparation process.

"content-particle size," such as 3% – 0.075 mm PUA. The 70# asphalt was heated to molten state by oven, and the PUA powder was added to the molten asphalt by three times. After the PUA powder was added, the asphalt was sheared and stirred with the high-speed shear apparatus, and the stirring process followed the principle of "low speed-high speed-low speed." After shearing and mixing, the modified asphalt was placed at room temperature, and the preparation of PUA-modified asphalt was completed after swelling.

## 2.2 Methodology

#### 2.2.1 LCSM

The fine microstructure of PUA particles (4–5 mm) was identified and analyzed by LCSM. The OLS4100 LCSM was used to characterize the microstructure. The characterization scales were 400, 200, and 100  $\mu$ m, and the characterization areas were the cross-section of granular materials, as shown in Figure 2.

#### 2.2.2 LPSA

The particle size distribution and composition characteristics of PUA powder after grinding were analyzed by LPSA. Before characterization, the materials were preliminarily divided into three grades of 0.075, 0.15, and 0.3 mm, and then, the laser particle size analysis was performed on the three types of PUA materials. Mastersizer 3000 LPSA was

used for laser particle size characterization. The powder material was dispersed with ethanol. The scanning frequency was 10 kHz and the particle size fraction was 100.

#### 2.2.3 SEM

Functional microstructure characterization using LYRA 3 XMU focused ion beam field emission scanning electron microscopy, magnification of 100–20,000 times. The PUA particles were amplified by 300–4,000 times. The PUA powder after grinding was amplified by 600–4,000 times and the modified asphalt with PUA modifier was amplified by 100–1,000 times, as shown in Figure 3 [24].

#### 2.2.4 Brookfield viscosity (physical property)

In this study, the Brookfield rotational viscometer (ASTM D 4402) [25] was used to analyze the influence of modifiers on the viscosity of asphalt at different temperatures. In this test, the rotor model was SC4-27, rotation speed was 20 rad/min, and the testing temperatures were 95, 115, 135, 150 and 175°C.

#### 2.2.5 The MSCR test

In this study, the MSCR test was used to evaluate the antirutting ability of the PUA-modified asphalt at high temperature. According to AASHTO T 350 [26], the test temperature was set to 64°C, the diameter of parallel plate was 25 mm, and the spacing was 1 mm. During the MSCR test,

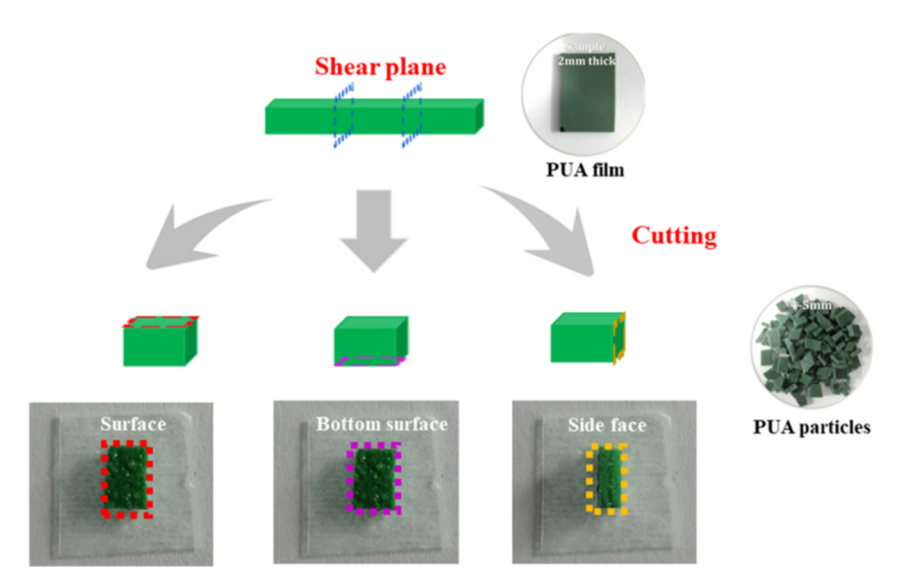


Figure 2: PUA material cutting method and LCSM characterization area.

the stress level contained 1.0 and 3.2 kPa, which would be repeated for 20 and 10 times, respectively. Every level included 10 cycles, which consisted of 1s creep stage and 9s unloading recovery stage per cycle that would last 300 s. The evaluating indices were recovery rate (R) and unrecoverable creep compliance ( $J_{\rm nr}$ ). The recovery rate ( $R_{0.1}$ ,  $R_{3.2}$ ), unrecoverable creep compliance ( $J_{\rm nr-diff}$ ) of each cycle were calculated by the following formulas. The calculation formula was mainly as follows:

$$R = (\gamma_{\rm p} - \gamma_{\rm nr})/(\gamma_{\rm p} - \gamma_{\rm 0}),$$
 (1)

$$J_{\rm nr} = (\gamma_{\rm nr} - \gamma_0)/\tau, \qquad (2)$$

$$J_{\text{nr-diff}} = \frac{(J_{3.2} - J_{0.1}) \cdot 100}{J_{3.2}},$$
 (3)

where  $\tau$  is the duration of each cycle;  $\gamma_p$  is the peak strain in each loading cycle;  $\gamma_{nr}$  is the residual strain in each loading cycle;  $\gamma_0$  is the initial strain for each loading cycle;  $\gamma_0$  is the unrecoverable creep compliance at 0.1 kPa stress level; and  $\gamma_{3.2}$  is the unrecoverable creep compliance at 3.2 kPa stress level.

#### 2.2.6 Linear amplitude sweep test

The testing temperature was set to 18°C, the diameter of parallel plate was 8 mm, and the spacing was 2 mm. Frequency sweep: Under strain control mode, the strain was 0.1%, sand weep frequency ranged from 0.2 to 30 Hz. Amplitude sweep: Under using strain control mode, sweep frequency was set to 10 Hz. First, 100 cycles were pre-loaded to the specimen under 0.1% strain. Then, the specimen was continuously loaded with 1% linear growing rate at 1–30% strain level. One hundred

cycles were loaded at each strain level and the total testing time was 310 s. The shear strain peak, shear stress peak, phase angle, and dynamic shear modulus were recorded every 10 repeated loads. According to the obtained stress—strain data, the simplified viscoelastic continuum damage (S-VECD) model was used for nonlinear fitting to obtain the damage characteristic curve of the PUA-modified asphalt.

#### 2.2.7 Time sweep test

The fatigue failure criterion of PUA-modified asphalt was determined by the time sweep test and the LAS test. For the time sweep test, the testing temperature was set to 18°C, same as the LAS test. The diameter of parallel plate was 8 mm and the spacing was 2 mm. The strain was controlled around 3% and the sweep frequency was 10 Hz. The loading time and dynamic shear modulus were recorded. The modulus loading time at 50% level was selected as the fatigue life of asphalt material.

## 3 Results and discussion

# 3.1 Microstructure characterization of PUA materials

# 3.1.1 Functional microstructure identification of PUA material

Figures 4–6 show the scanning images of PUA particles at three scales of 400, 200, and 100 µm by laser and height

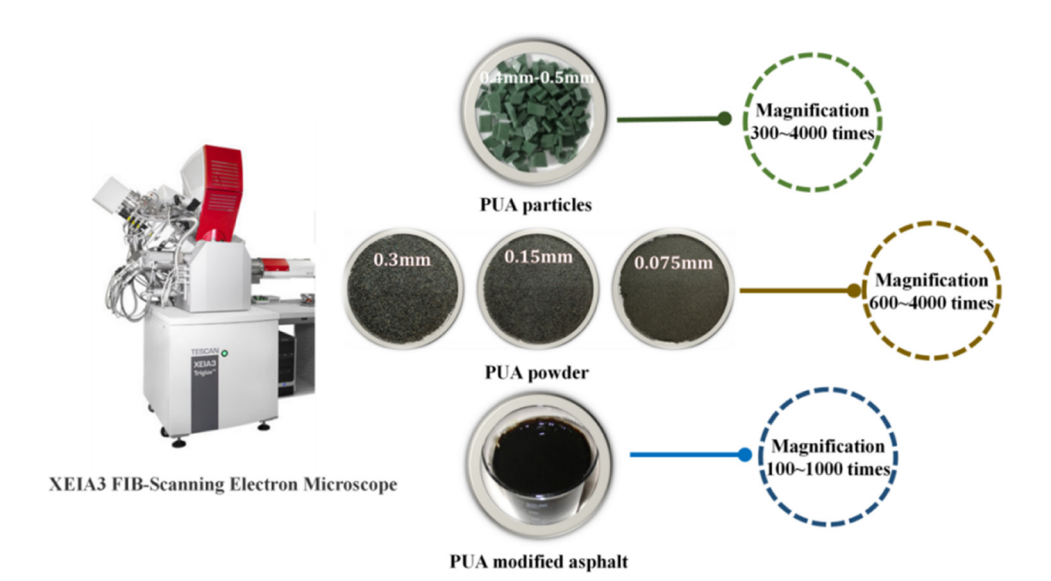


Figure 3: SEM characterization plan.

6 — Xiaolong Sun et al. DE GRUYTER

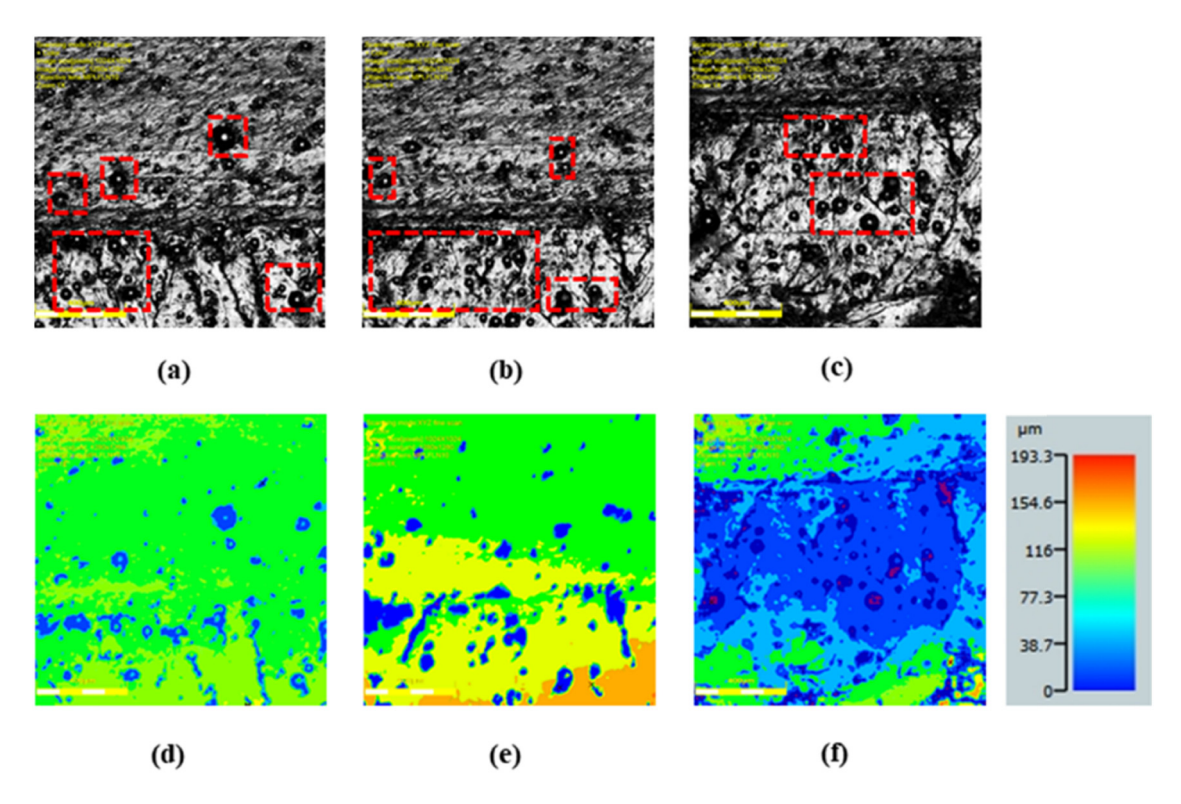


Figure 4: 400 µm characterization results: (a) Zone1-laser; (b) Zone2-laser; (c) Zone3-laser; (d) Zone1-axis depth; (e) Zone2-axis depth; and (f) Zone3-axis depth.

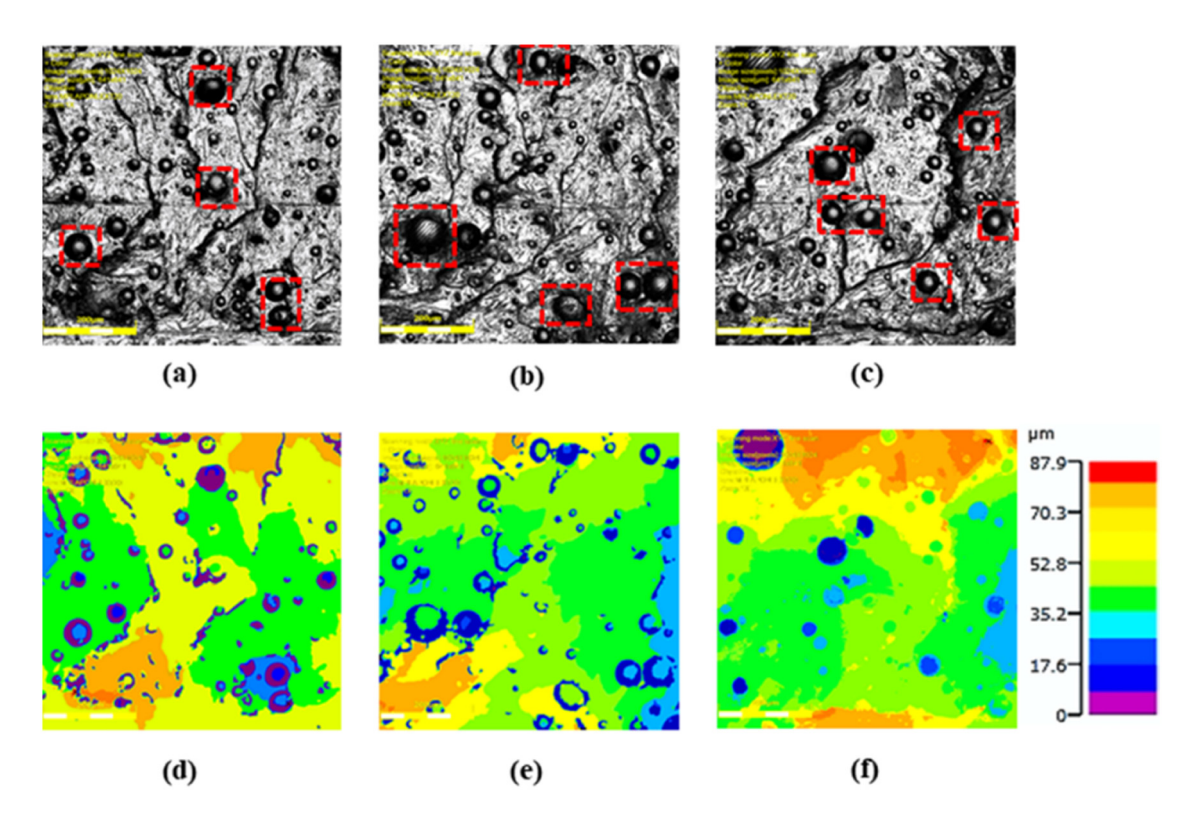


Figure 5: 200 µm characterization results: (a) Zone1-laser; (b) Zone2-laser; (c) Zone3-laser; (d) Zone1-axis depth; (e) Zone2-axis depth; and (f) Zone3-axis depth.

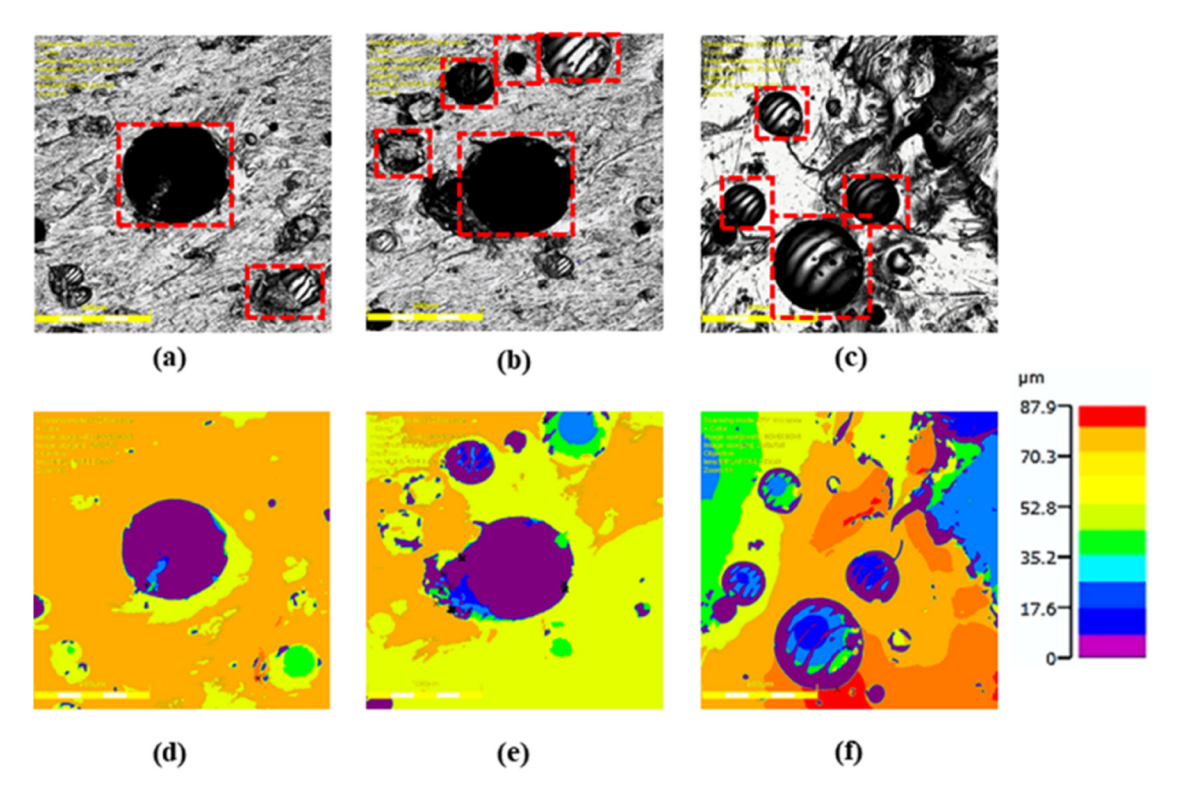


Figure 6: 100 µm characterization results (a) Zone1-laser; (b) Zone2-laser; (c) Zone3-laser; (d) Zone1-axis depth; (e) Zone2-axis depth; and (f) Zone3-axis depth.

projection respectively. The results implied that there were lots of spherical structures with different sizes in the cross-section of PUA particles, which existed independently in the cross-section. The spherical structures with different sizes could form triangular structures, which improved the stress absorption and dispersion effect of PUA materials when subjected to external force. Therefore, it could be speculated that the high elastic properties of PUA modifier might not only come from the properties of the spherical structure but also come from the interaction between the spherical structures. The microstructure was further expanded, as shown in Figures 5 and 6. From Figure 5a-c, it could be known that the diameter of the spherical structure ranged from 3 to 110 µm and the structural shape was complete. The spherical functional structure exhibited the quasi-circular feature in the planar region, but some spherical structures deformed at the boundary position. Figures 4g-i, 5g-i, and 6g-i show the 2D depth projection of PUA particle cross-section. According to these results, the spherical structure in the PUA particle section was concave structure with high around and low middle, and the concave depth of different spherical structures was totally different. Some spherical structures were interlaced with each other, resulting in dislocation contact in space. When the PUA material surface was subjected to external

load, the spherical structure contacted on both sides would be indirectly affected by the middle spherical structure, so as to absorb and disperse the stress and improve the bearing capacity of PUA materials.

#### 3.1.2 Microstructure of PUA particles

Figure 7a-c shows the SEM images of PUA materials at different magnifications. ImageJ graph processing software was used to characterize the diameter of the ball structure in Figure 7c, and the results are shown in Figure 8. According to Figures 7 and 8, there were many round holes in the cross-section of PUA particles and the diameters of most hole structures were within the range of 15–25 µm. The diameters of a small amount of the hole structures were less than 10 µm or greater than 30 µm. Different holes existed independently and the boundary was relatively smooth. The internal part of the hole structure presented the black background, while the background of other hole structures was relatively shallow, which indicated that there were also differences in the depth of different hole structures. The pore structures with different diameters were evenly distributed in PUA materials and there was a certain regional combination

between them, which might be the reason why PUA materials had high elastic properties [27].

# 3.2 Particle size composition and microstructure of PUA powder

#### 3.2.1 Particle size composition of PUA powder

The laser particle size analysis results of PUA powder material (0.075, 0.15, and 0.3 mm) are shown in Figure 9. It could be obtained that the particle size distribution of three grades of PUA powder presented normal distribution. The particle size composition of 0.075 mm PUA powder was relatively continuous and the particle size composition range was approximately within  $0.1–300\,\mu m$ . The particle size of

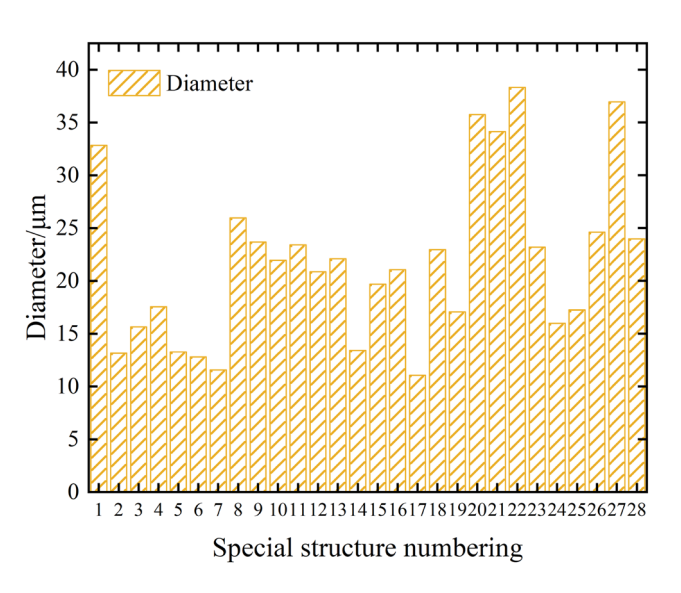


Figure 8: Diameter distribution of special structures.

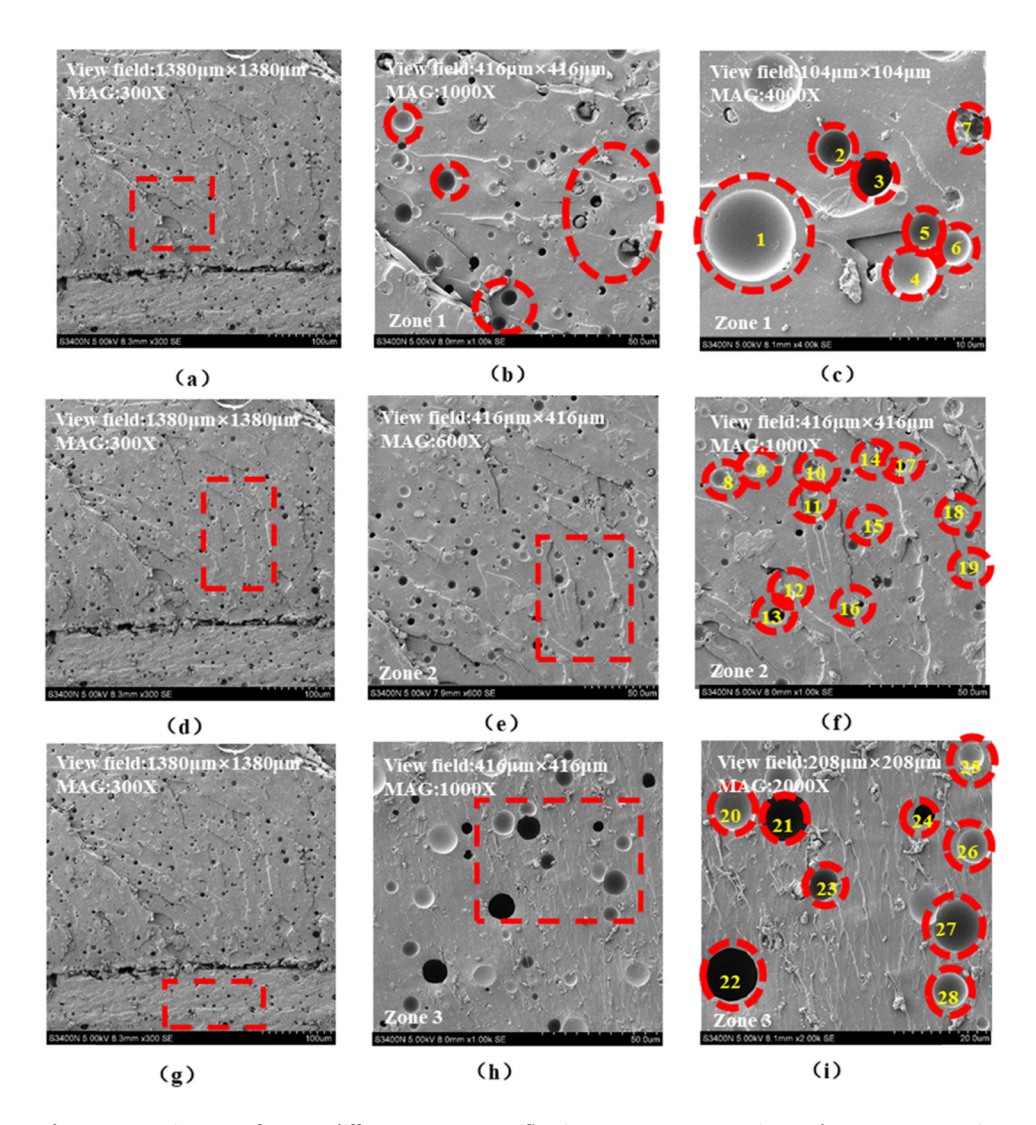


Figure 7: SEM images of PUA at different MAG (magnification): (a) Zone 1–300 times; (b) Zone 1–1,000 times; (c) Zone 1–4,000 times; (d) Zone 2–300 times; (e) Zone 2–600 times; (f) Zone 2–1,000 times; (g) Zone 3–300 times; (h) Zone 3–1,000 times; and (i) Zone 3–2,000 times.

90% PUA powder was in the range of  $13-215\,\mu m$  and the particle content of  $100\,\mu m$  was the highest, about 7.7%. The particle size distribution of  $0.15\,m m$  PUA powder with 90% volume content was within  $100-400\,\mu m$ . The particle size of the PUA powder with the highest content was  $200\,\mu m$  and the content was about 12%. When the particle size of  $0.3\,m m$  PUA powder was in the range of  $400-1,000\,\mu m$ , its composition was not continuous and some particle sizes were missing.

#### 3.2.2 Micro morphology of PUA powder

The SEM results with different magnifications are shown in Figure 10. PUA particle size of 0.075 mm was between 0.02 and 0.04 mm and the particles were relatively smooth. There were a small number of grooves with spherical structure on the surface of the particles and a small number of PUA particles with small particle sizes were mixed inside the grooves. The spherical structures in SEM images were

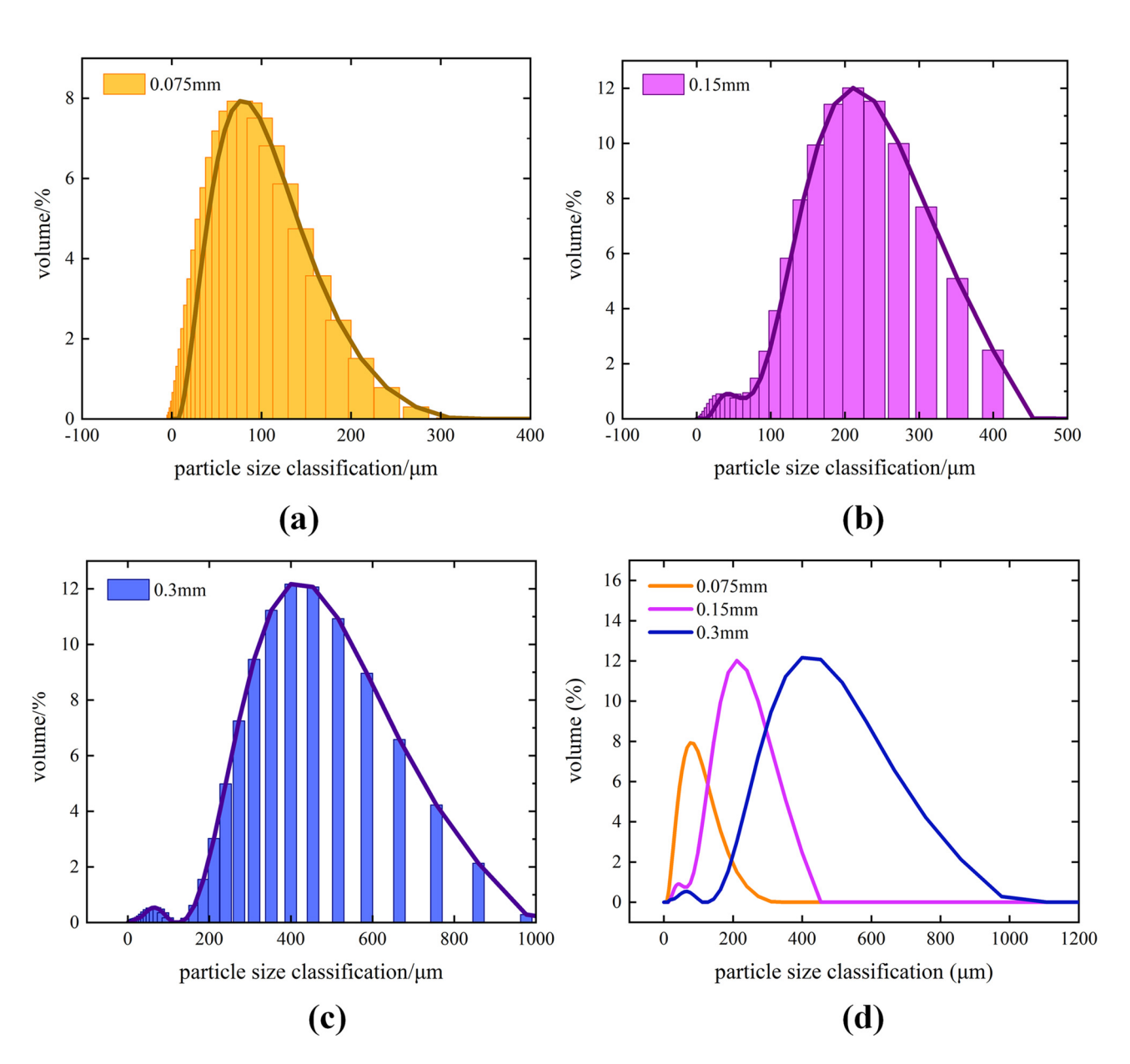


Figure 9: Laser particle size analysis results: (a) 0.075 mm PUA; (b) 0.15 mm PUA; (c) 0.3 mm PUA; and (d) PUA particle size composition comparison.

10 — Xiaolong Sun et al. DE GRUYTER

presented with the results of fine grinding [28]. These spherical structures improved the stress absorption and dispersion effect of PUA materials under external force and might upgrade the mechanical properties of PUA-modified asphalt. PUA particle size of 0.15 mm was between 0.1 and 0.2 mm. The shape of particles was irregular and the edges were clear. There were a small number of grooves with spherical structure on the surface of PUA powder. Compared with 0.075 mm PUA particles and 0.15 mm PUA particles, the surface of 0.3 mm PUA powder was rougher and there were also a small number of grooves with spherical structure.

## 3.3 Microstructure of PUA-modified asphalt

Figure 11 shows the interface between PUA of different particle sizes and 70# asphalt. According to Figure 11a–c, the PUA of 0.075 mm particle size was embedded in the asphalt. The interaction section between PUA and 70# asphalt was the relatively flat homogeneous structure with no obvious pores and cracks and the surface bonding state was relatively excellent. Therefore, it could be explained that when the PUA-modified asphalt was damaged by external force, PUA would absorb part of the load and perform the

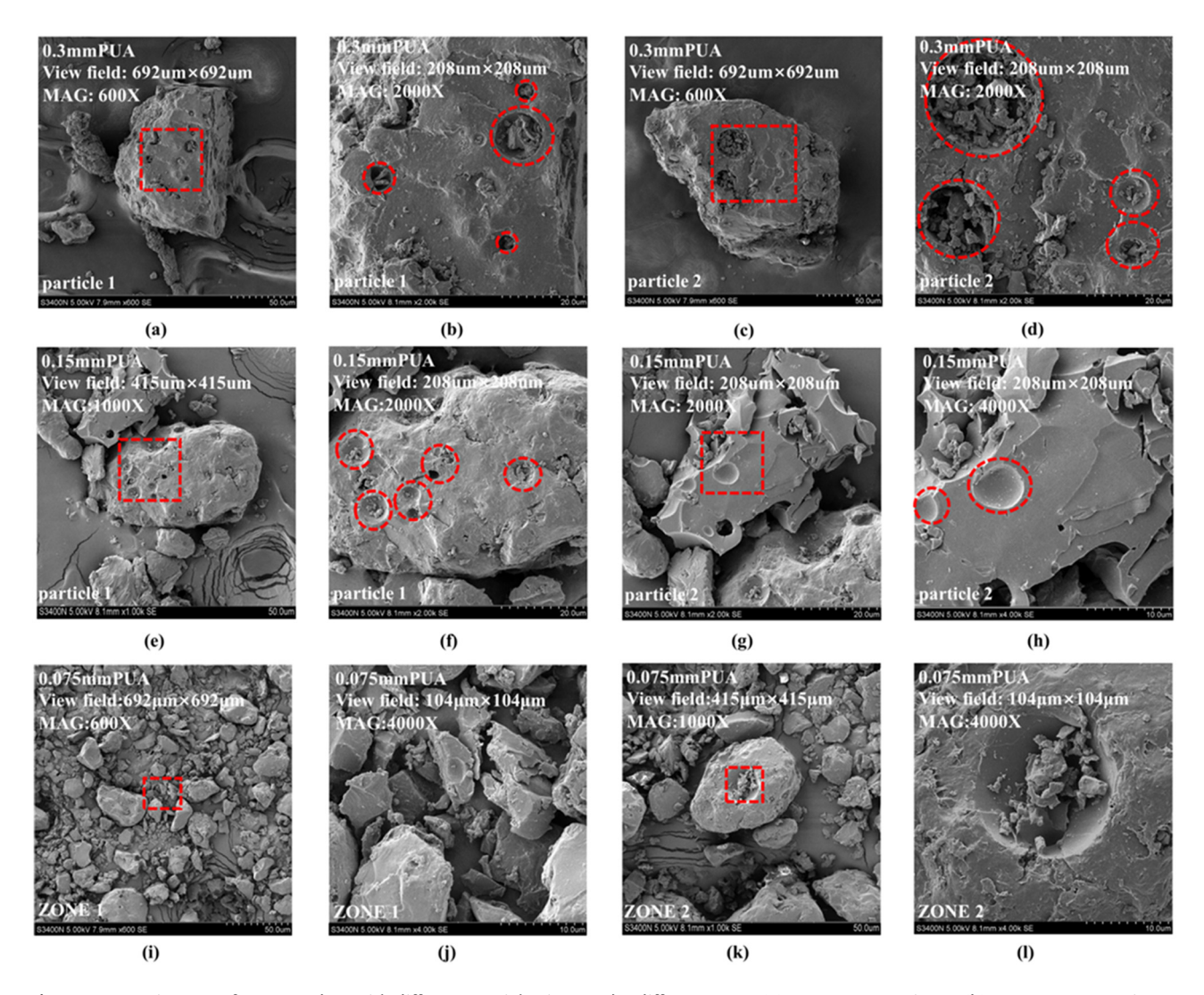


Figure 10: SEM images of PUA powders with different particle sizes under different MAG: (a) 0.3 mm - 600 times; (b) 0.3 mm - 2,000 times; (c) 0.3 mm - 600 times; (d) 0.3 mm - 2,000 times; (e) 0.15 mm - 1,000 times; (f) 0.15 mm - 2,000 times; (g) 0.15 mm - 2,000 times; (h) 0.15 mm - 4,000 times; (i) 0.075 mm - 600 times; (j) 0.075 mm - 4,000 times; (k) 0.075 mm - 100 times; and (l) 0.075 mm - 4,000 times.

effect of stress transfer [29]. According to Figure 11d-f, when the particle size of PUA increased to 0.15 mm, there were many folds and pores between PUA and 70# asphalt binder surface and they were not closely integrated, which indicated that 0.15 mm PUA-modified asphalt was the heterogeneous system. 0.15 mm PUA particles could not be completely dissolved in asphalt but filled in asphalt as elastic particles. According to Figure 11g-i, when the particle size of PUA increased to 0.3 mm, the cracks on the interface between PUA and 70# asphalt were deepened and the wrinkles were increased. Therefore, excessive PUA particles would limit the overall fluidity of the modified asphalt, so that the ability of the composite system to resist external forces became weak [29-31]. In summary, with the gradual increase of PUA particle size, the cracks and folds of the interface between PUA particles and 70# asphalt increased gradually, resulting in poor adhesion of the interface. However, 0.075 mm PUA particles had the excellent combination with matrix asphalt, which demonstrated that the interface was clear and the transition was obvious. Therefore, it could improve the viscoelastic mechanical properties of modified asphalt greatly.

## 3.4 Rheological properties

#### 3.4.1 Brookfield viscosity analysis

The Brookfield viscosity results of different types of PUAmodified asphalt and matrix asphalt at 90, 115, 135, 150, and 175°C are presented in Figure 12. According to Figure 12, the apparent viscosity of different types of asphalt decreased with the increase in temperature, and the varying trend was basically the same. PUA modifier could raise the viscosity of asphalt at different temperatures. When the testing temperature was higher than 150°C, the apparent viscosity gap between different asphalts was small.

Figure 13 presents the Brookfield viscosity curves of modified asphalt with different PUA dosage/fineness. The results implied that under different temperature conditions, asphalt viscosity increased gradually as PUA content enlarged. Compared with 70# asphalt, the viscosity of 3, 6, and 9% PUA-modified asphalt increased by 48, 53, and 60% at 90°C, respectively. When the testing temperature raised to 115°C, the viscosity of 3, 6, and 9% PUA-

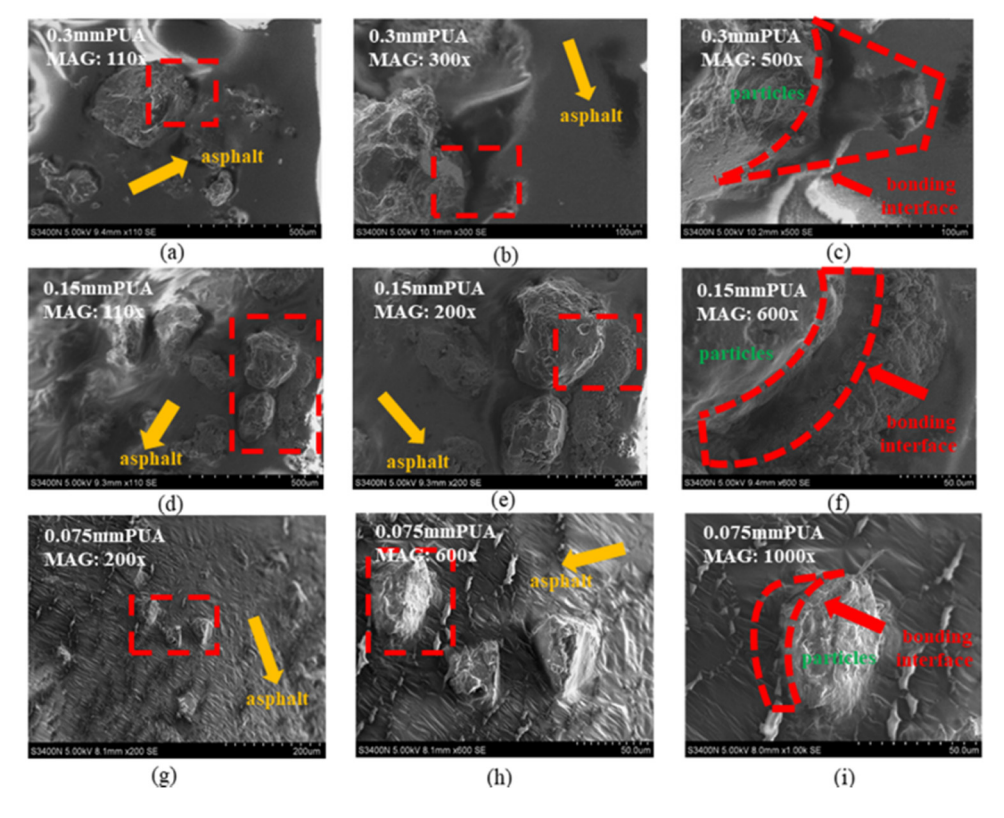


Figure 11: SEM images of different PUA-modified asphalt under different MAG: (a) 0.3 mm - 110 times; (b) 0.3 mm - 300 times; (c) 0.3 mm -500 times; (d) 0.15 mm - 110 times; (e) 0.15 mm - 200 times; (f) 0.15 mm - 600 times; (g) 0.075 mm - 200 times; (h) 0.075 mm - 600 times; and (i) 0.075 mm - 1,000 times.

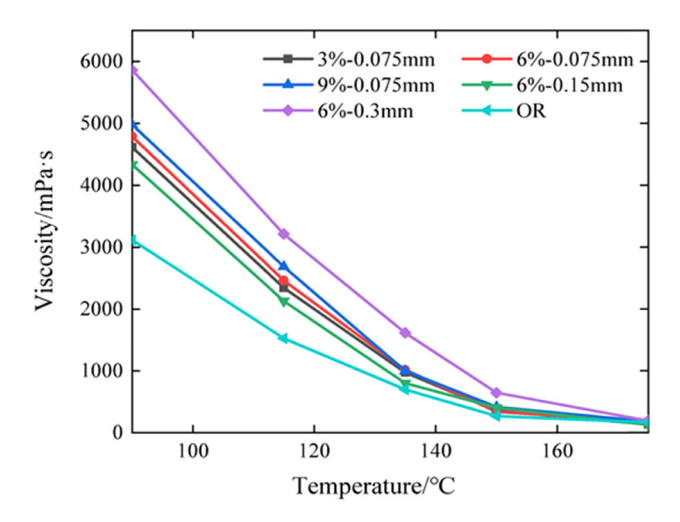


Figure 12: Brookfield viscosity results of PUA-modified asphalt.

modified asphalt increased by 53, 61, and 76%, respectively. When the temperature was over 130°C, the apparent viscosity of modified asphalt and matrix asphalt was almost the same, which indicated that PUA could increase the viscosity of asphalt when temperature below 130°C. This might be because the molecular bond generated by the interaction between PUA and asphalt enhanced the force between asphalt molecules, thereby leading to the apparent viscosity increase of asphalt [32]. When temperature was above 130°C, the improving effect of PUA on the viscosity of asphalt was not obvious. Figure 4b illustrates that during the gradual increase of PUA particle size, the viscosity of asphalt represented the varying trend of first decrease-then increase. 0.075 mm PUA modifier had excellent effect on viscosity improvement, while the enhancing impact of 0.15 mm PUA modifier was low,

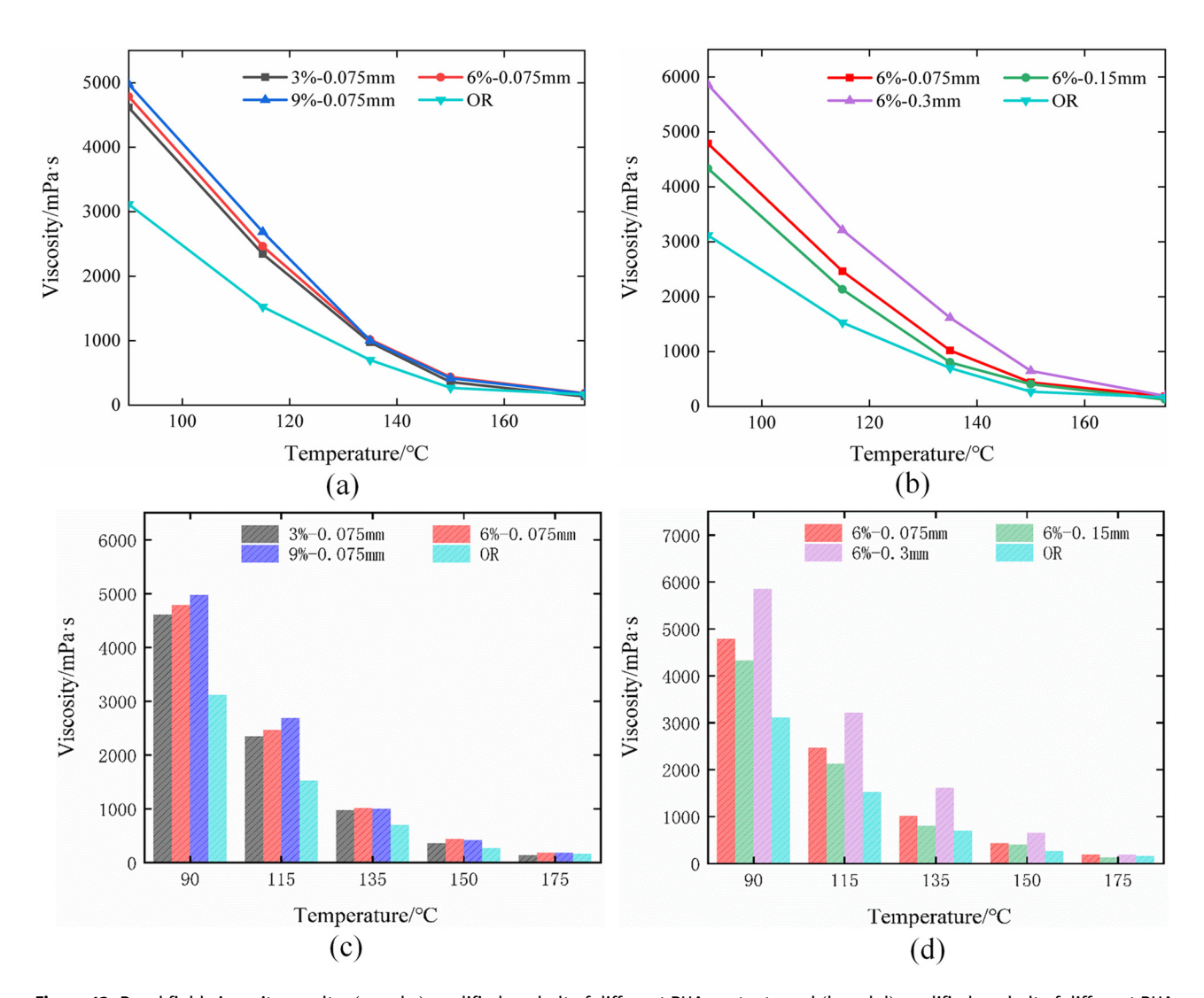


Figure 13: Brookfield viscosity results: (a and c) modified asphalt of different PUA contents and (b and d) modified asphalt of different PUA particle sizes.

which might be affected by the dispersion state of PUA powder inside asphalt. The molecular bonds generated by the interaction between PUA and asphalt strengthened the force between asphalt molecules, which raised the viscosity of asphalt. The compatibility between PUA of large particle size and asphalt was degraded, which destroyed the original structure of asphalt and led to the decrease of asphalt viscosity. However, the apparent viscosity of 0.3 mm PUA-modified asphalt was maximum, which was due to the blocking force of PUA particle of large size on the rotor leading to the testing result error [32].

#### 3.4.2 MSCR analysis

#### 3.4.2.1 MSCR test result

Figure 14 demonstrates the MSCR testing results of PUA-modified asphalt and matrix asphalt. Under the testing condition of 0.1 kPa and 64°C, the strain of different types of PUA-modified asphalt increased in varying degrees. In the unloading stage, the strain rebound obviously. Under the condition of 3.2 kPa stress level, the strain amplitude of asphalt was large and the strain rebound of asphalt was not obvious in the unloading stage. Based on this, the recovery rate  $R_{0.1}$ , the unrecoverable creep compliance

 $J_{\rm nr0.1}$  in 0.1 kPa load cycle, the recovery rate  $R_{3.2}$ , the unrecoverable creep compliance  $J_{\rm nr3.2}$  in 3.2 kPa load cycle, and stress sensitivity coefficient  $J_{\rm nr-diff}$  were calculated as the study indices of MSCR. The calculated results of study indices are plotted as Figure 15.

Figure 15a and b shows that compared with 70# asphalt,  $R_{0.1}$  and  $R_{3.2}$  of different modified asphalt increased obviously, while  $J_{\rm nr0.1}$  and  $J_{\rm nr3.2}$  decreased, which suggested that PUA modifier could reduce the cumulative deformation of asphalt under cyclic loading and improve the elastic recovery performance of asphalt. This might be because that PUA material belonged to elastomer and could react with some component of asphalt resulting in colloid composition variation of asphalt. Figure 15c shows that  $J_{\rm nr-diff}$  of 3% – 0.075 mm PUA-modified asphalt was smaller than that of 70# asphalt, which supposed that 3% – 0.075 mm modifier could reduce the stress sensitivity of asphalt. That might be due to the great fusion between fine PUA particles and asphalt, which reduced the sensitivity of modified asphalt to the variation of stress level [10].

# 3.4.2.2 Effect of PUA content on creep properties of asphalt at high temperature

Figure 16 shows the MSCR test results of modified asphalt with different PUA contents and matrix asphalt. According

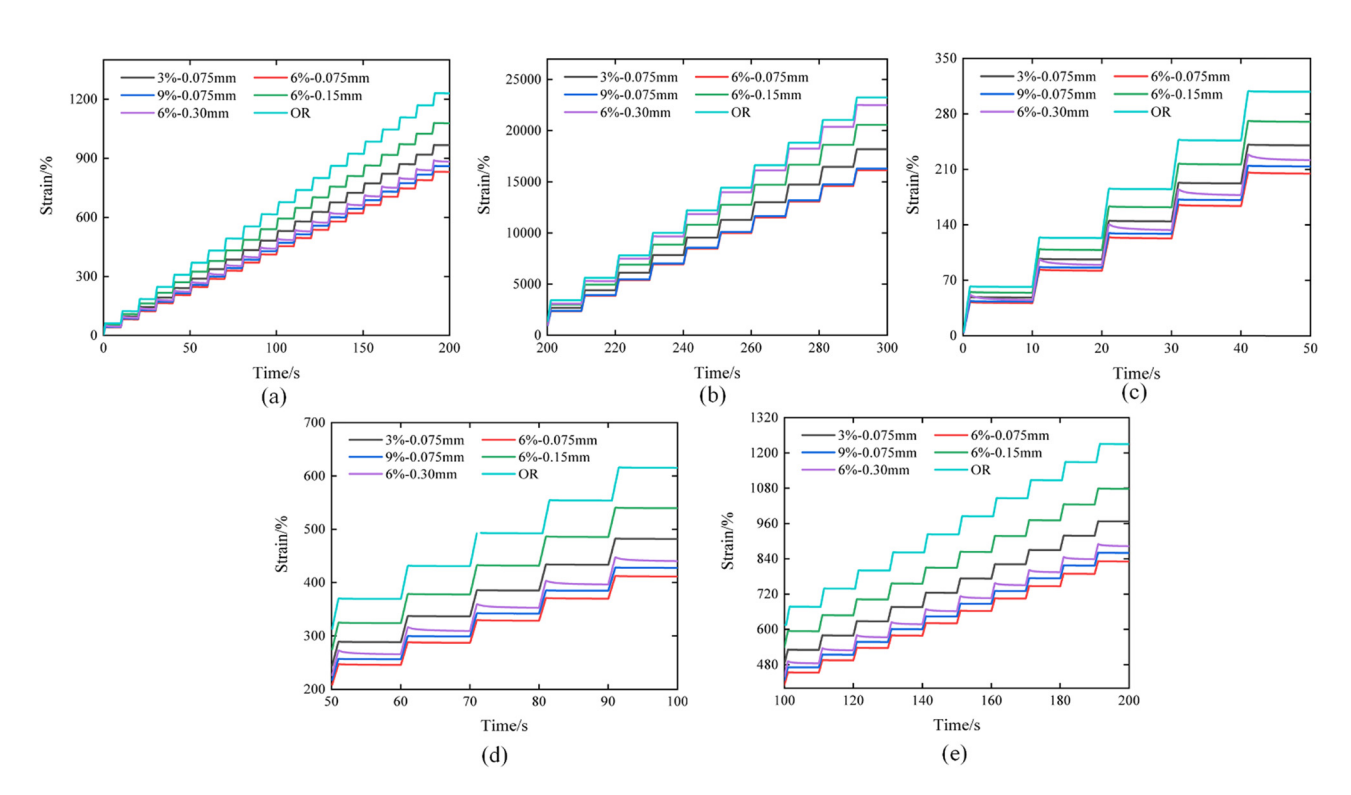


Figure 14: MSCR test results: (a) 0.1 kPa stress level/0-200 s; (b) 3.2 kPa stress level/200-300 s; (c) 0.1 kPa stress level/0-50 s; (d) 0.1 kPa stress level/0-100 s; and (e) 0.1 kPa stress level/0-200 s.

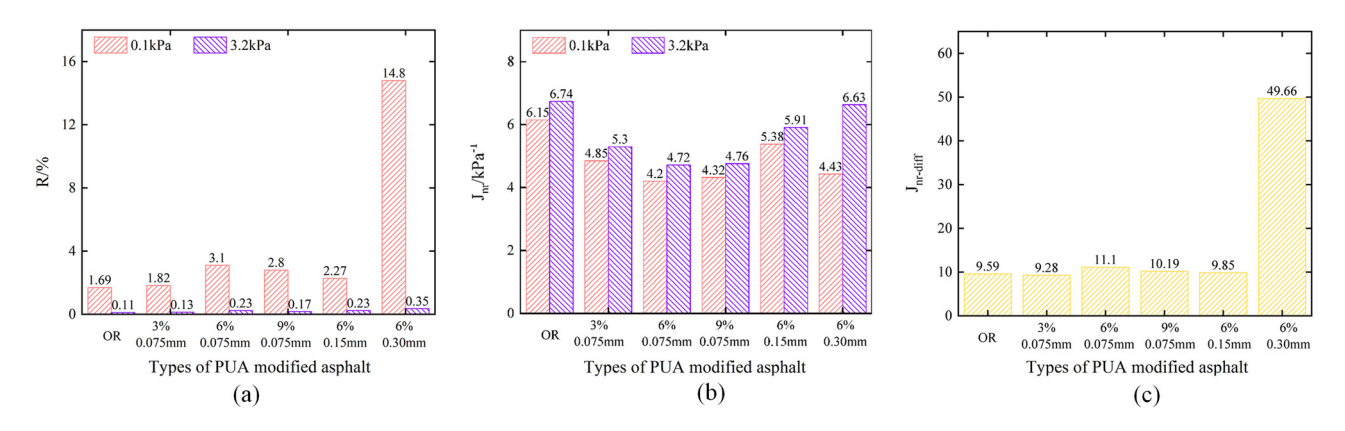


Figure 15: Calculated evaluating indices of MSCR test: (a) recovery rate; (b) unrecoverable creep compliance; and (c) stress sensitivity coefficient.

to Figure 16a and b, under different stress conditions, the cumulative strain of modified asphalt was smaller than that of 70# asphalt, and with the increase in the PUA content, the cumulative strain of asphalt decreased first and then increased. According to Figure 16, it could be analyzed that under different stress conditions, the cumulative strain of modified asphalt was smaller than that of 70# asphalt. According to Figure 16c and d, under stress levels of 0.1 kPa, the recovery rate of PUA-modified asphalt increased from 1.69 to 3.1% when dosage rose from 0 to

6%. The *R* peaked at PUA dosage of 6%. When the PUA dosage continued rising, the *R* of PUA-modified asphalt decreased slightly, from 3.1 to 2.8%, which indicated that appropriately increasing the dosage within a certain range could improve the elastic resilience of modified asphalt and reduce the cumulative strain of asphalt. But the modifying effect of PUA would be weaken while the dosage was over rational range. The modifying effect might be related to the reason that PUA modifier could adsorb aromatic and saturated components of asphalt and improve

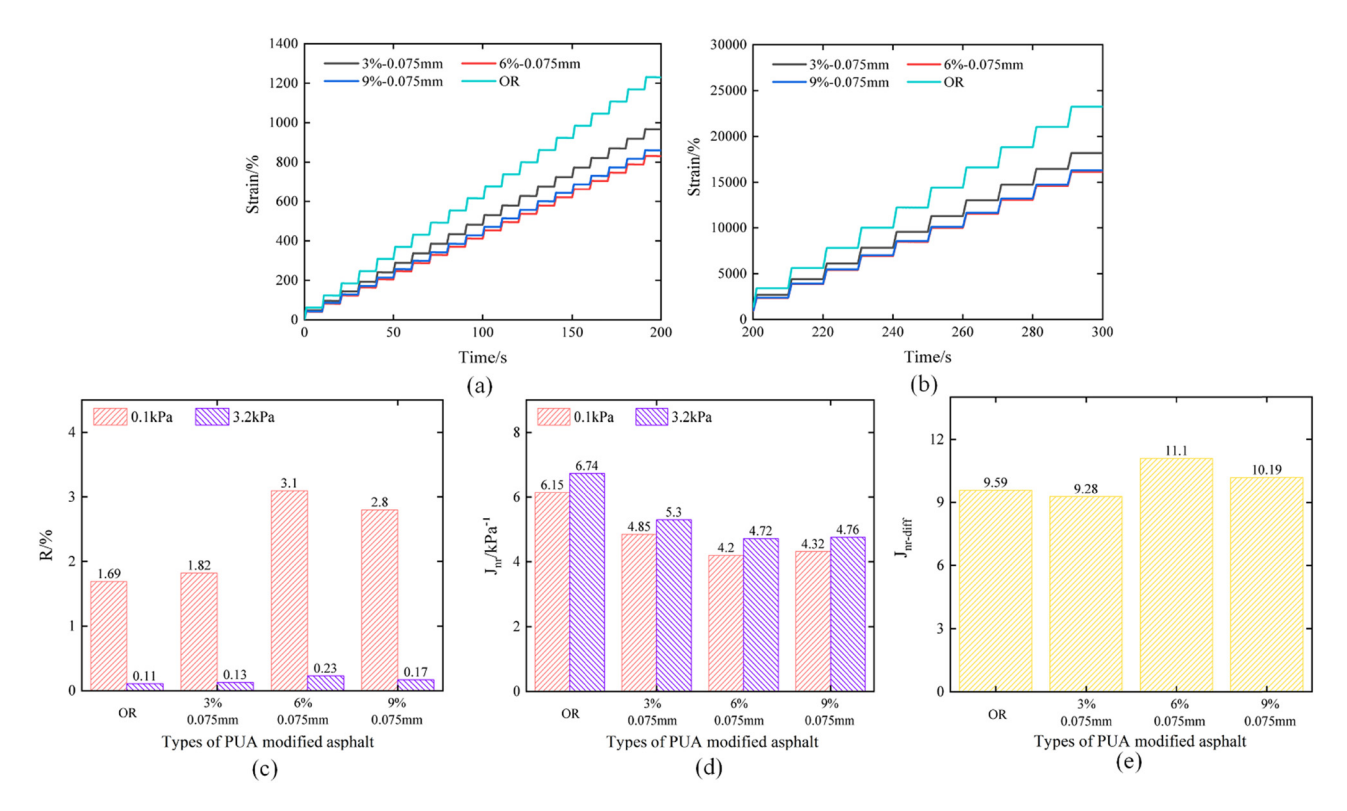


Figure 16: Different contents of PUA: (a) 0.1 kPa stress level; (b) 3.2 kPa stress level; (c) recovery rate; (d) unrecoverable creep compliance; and (e) stress sensitivity coefficient.

the viscoelasticity of asphalt during the fusion process [16]. Reasonable dosage of PUA could act synergistically in asphalt to form a more stable particle structure system. However, excessive dosage of PUA modifier might exceed the dispersion limit of asphalt carrier, resulting in the poor agglomeration and dispersion of PUA inside asphalt, which led to the deterioration of modification effect [33,34]. Figure 16e illustrates that  $J_{\rm nr-diff}$  of PUA-modified asphalt was basically larger than that of 70# asphalt, because PUA modifier could mitigate the stress sensitivity of asphalt at high temperature.

# 3.4.2.3 Effect of PUA particle size on creep properties of asphalt at high temperature

It could be investigated from Figure 17a and b that under the stress level of 0.1 kPa, the cumulative strain variation in modified asphalt followed the changing rule of increases—decreases as particle size was amplified, while at the stress level of 3.2 kPa, the cumulative strain of asphalt kept increasing following the increase in particle size. While the particle size increased from 0.075 to 0.15 mm, the recovery rate of PUA-modified asphalt decreased by 27%, and the unrecoverable creep compliance increased by 28%, the elastic recovery performance of asphalt

degraded obviously. The degradation was related to the fusion and dispersion of PUA in asphalt. The increased particle size of PUA reduced the specific surface area, which abated the development of structure asphalt [14]. When the particle size increased from 0.15 to 0.3 mm, the recovery rate increased by 552%, and the unrecoverable creep compliance decreased by 18%. The sudden increase in recovery rate might originate in the PUA material instead of asphalt, which led to the testing error of recovery rate. Actually, the recovery rate of 0.3 mm PUA material-modified asphalt might be still decreased. Under the stress level of 3.2 kPa, the recovery rate and unrecoverable creep compliance of different modified asphalt were small, which was around 0.2%. Figure 17e demonstrates that the  $J_{\text{pr-diff}}$  of 0.075 and 0.15 mm PUA-modified asphalt was similar to that of 70# asphalt. However, the  $J_{\text{nr-diff}}$  of 0.3 mm PUA-modified asphalt increased sharply, which was related to the experimental error of *R*.

#### 3.4.3 Time sweep analysis

#### 3.4.3.1 Time scanning test result

Figure 18 shows the time-complex shear modulus curve. Under the controlled strain mode, the complex shear

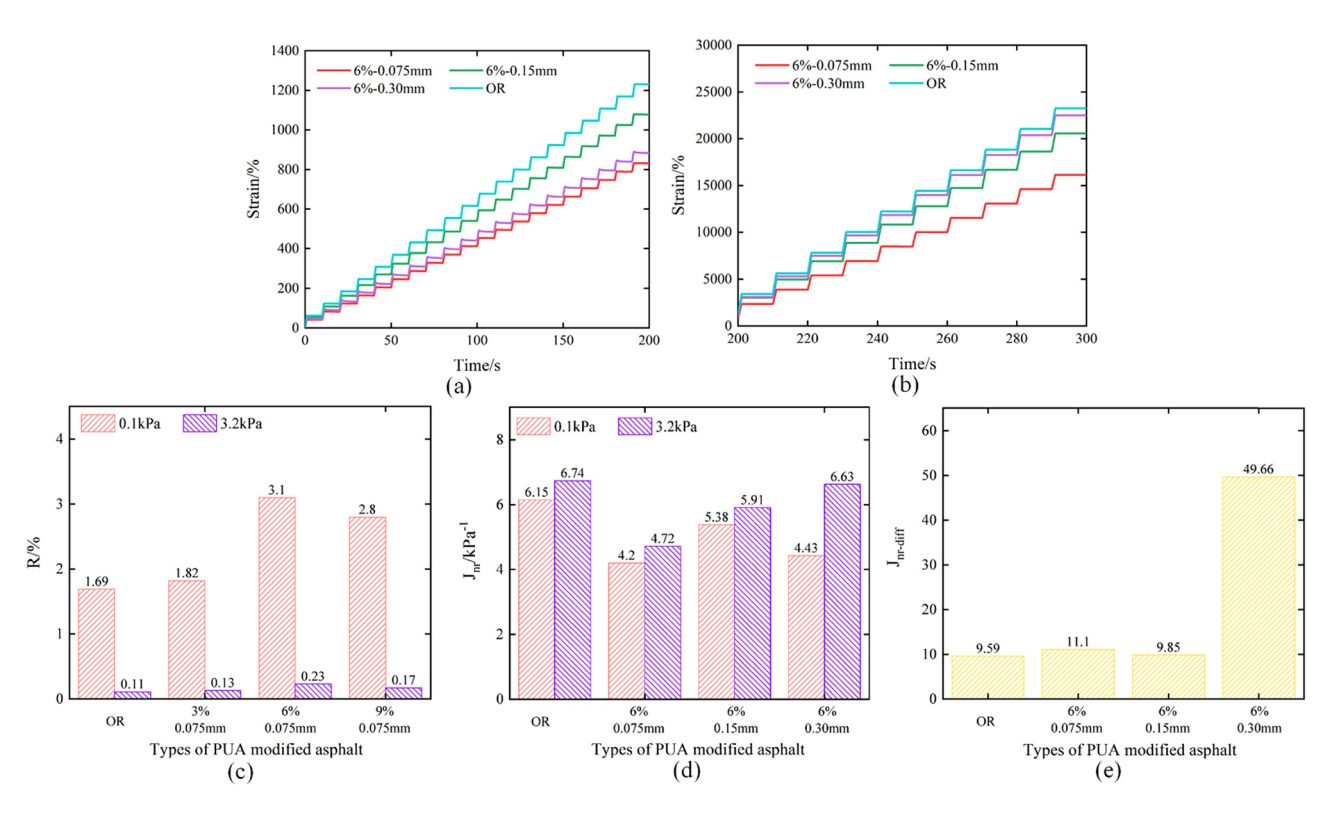


Figure 17: Different particle sizes of PUA: (a) 0.1 kPa stress level; (b) 3.2 kPa stress level; (c) recovery rate; (d) unrecoverable creep compliance; and (e) stress sensitivity coefficient.

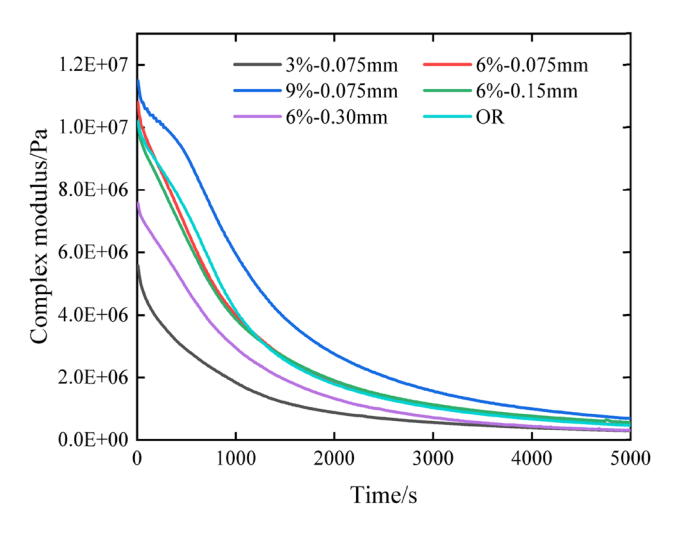


Figure 18: Time sweep test results of PUA-modified asphalt.

modulus of different PUA-modified asphalt decreased gradually as time went on, and the state of asphalt transformed from elasticity to viscous flow, which experienced the process of "fatigue loss accumulation-microcracks generation-fatigue failure" [35]. When the complex shear modulus decreased to 50% of the initial modulus, the curve tended to be flat. The initial modulus  $G_1^{\star}$  of different PUA-modified asphalt, the modulus value  $G_2^{\star}$  when the initial modulus reduced to 50%, the corresponding loading times  $N_{\rm fSO}$ , and the loading times  $N_{\rm fG}$  when the initial modulus reduced to 41–44% were calculated and selected as study indices. The calculated results are shown in Table 2.

From Table 2, it could be analyzed that the  $G_1^*$  of 9% – 0.075 mm PUA asphalt and 6% – 0.075 mm PUA asphalt were larger than that of 70# asphalt, while the  $G_1^*$  of other modified asphalts were smaller than that of matrix asphalt. The results showed that the initial elasticity of 9% – 0.075 mm PUA asphalt and 6% – 0.075 mm PUA asphalt was higher than that of 70# asphalt. When the fatigue life of

Table 2: Fatigue life of PUA-modified asphalt

	<b>G</b> <sub>1</sub> * (kPa)	G <sub>2</sub> * (kPa)	N <sub>f50</sub> (times)	N <sub>fG</sub> (times)
OR	10,234	4,396	8,280	9,480
3% - 0.075 mm	5,570	2,780	5,500	7,500
6% - 0.075 mm	10,800	5,400	7,020	8,580
9% - 0.075 mm	11,500	5,740	10,380	12,420
6% - 0.15 mm	10,200	5,110	7,200	8,880
6% - 0.30 mm	7,570	3,780	7,380	9,180

asphalt was defined according to  $N_{\rm f50}$  and  $N_{\rm fG}$ , the fatigue life of asphalt increased gradually with the increase in PUA content. Regarding particle size, the increase in PUA particle size would lead to the degradation of the fatigue life of PUA-modified asphalt.

# 3.4.3.2 Effect of PUA content on mesothermal fatigue performance of asphalt

Time sweep test results of modified asphalt with different contents of PUA are shown in Figure 19a illustrating that the initial modulus of PUA-modified asphalt was lower than that of matrix asphalt when PUA dosage was 3%. The results contradicted the testing results of MSCR. With the rising of PUA content, the initial modulus of asphalt increased gradually, and the elastic modifying effect of PUA on asphalt raised gradually. Figure 19b and c demonstrates that the increase in the PUA content could promote the rising of  $G_1^*$  and  $G_2^*$ . Furthermore, the  $N_{f_{50}}$  and  $N_{f_{6}}$  also increased gradually, which could be concluded that PUA could improve the fatigue life of asphalt material. When the PUA content reached 9%, the fatigue performance of asphalt was improved obviously. The enhancing effect of PUA on fatigue life might be related to the impact of PUA on the viscoelasticity of asphalt, which might be because that the polyurethane elastomer could absorb

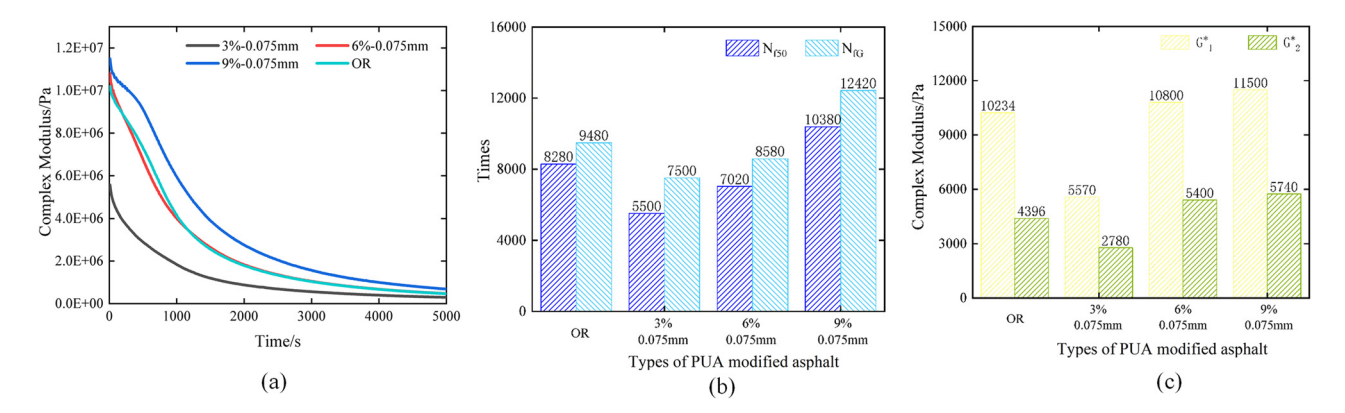


Figure 19: Different contents of PUA: (a) complex modulus; (b)  $N_{f50}$  and  $N_{fG}$ ; and (c)  $G_1^*$  and  $G_2^*$ .

more aromatic and oil components in asphalt, increasing the viscoelastic components of asphalt [17].

# 3.4.3.3 Effect of PUA particle size on mesothermal fatigue performance of asphalt

The time sweep test results of modified asphalt with different particle sizes of PUA are shown in Figure 11. It could be known from Figure 11 that except for 6% -0.075 mm PUA-modified asphalt, the initial modulus of PUA-modified asphalt was below that of 70# asphalt. The initial modulus of asphalt decreased with the increase in PUA particle size. Furthermore, with the decrease in PUA particle size, the change in  $N_{\rm f50}$  and  $N_{\rm fG}$  was not obvious and the fatigue life of PUA modified was slightly worse than 70# asphalt, which was contrary to the excellent modifying effect of PUA. Thus, time sweep test, as a traditional method for judging the fatigue performance of asphalt, was not suitable to evaluate the modifying effect of PUA on asphalt. Therefore, the mesothermal fatigue performance of asphalt would be further studied and compared based on the LAS test in the following section. However, some studies had shown that time sweep, as a traditional method for judging the fatigue performance of asphalt, lacked sufficient theoretical connection that could not well reflect the fatigue performance of asphalt [36-38]. Therefore, the mesothermal fatigue performance of asphalt would be further studied and compared based on the LAS test in the following section (Figure 20).

#### 3.4.4 LAS test analysis

#### 3.4.4.1 LAS test result

Figure 21 demonstrates the LAS test results of PUA-modified asphalt. According to the stress-strain relationship

diagram, the curve was divided into three stages, as shown in Figure 22. According to the AASHTO TP 101-14 [39], the peak stress was defined as the fatigue failure point of materials, namely the yield stress. The greater the yield stress was, the stronger the deformation resistance of the material would be. From Figures 21a and 22, all the stress peak values of PUA-modified asphalts were higher than that of matrix asphalt, which supposed that the PUA modifier could improve the deformation resistance of asphalt. Figure 21b shows that when the strain was 0, the curves of PUA-modified asphalt were below that of 70# asphalt. The comparison analysis of the initial phrase angle indicated that the polyurethane elastomer in PUA material had high hardness and elastic modulus, which changed the viscoelasticity of asphalt and improved the elastic composition of asphalt [16]. When the strain continued increasing, the phase angle reached the peak. In the final stage of the curve, the phase angles of 3% – 0.075 mm PUA-modified asphalt, 6% - 0.075 mm PUAmodified asphalt and 9% - 0.075 mm PUA-modified asphalt fluctuated, which made the rheological properties of modified asphalt become very complex. Therefore, the peak value of phase angle was suitable for fatigue failure judgment of 70# asphalt instead of PUA-modified asphalt [40]. Thus, to better analyze the stress variation in PUA-modified asphalt, the relevant data are calculated and detailed in Figure 23.

From Figure 23b, it could be analyzed that the yield strains of 3% – 0.075 mm PUA-modified asphalt and 6% – 0.075 mm PUA-modified asphalt were higher than those of 70# asphalt by 19 and 10%. The yield strains of 9% – 0.075 mm PUA-modified asphalt and 6% – 0.15 mm PUA-modified asphalt were lower than those of 70# asphalt by 5 and 10%, respectively. It could be preliminarily judged that 3% – 0.075 mm PUA modifier and 6% – 0.075 mm PUA modifier could effectively enhance the anti-deformation

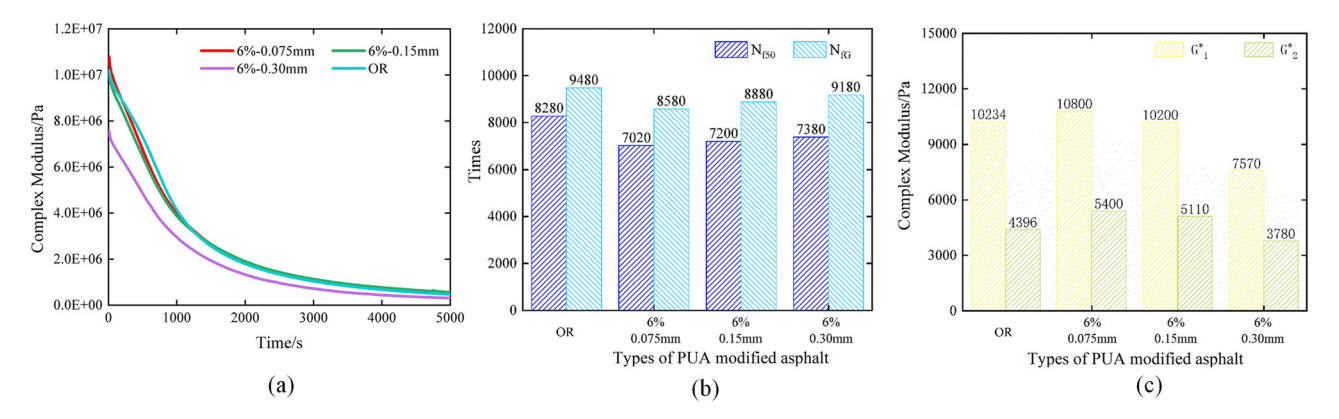


Figure 20: Different particle sizes of PUA: (a) complex modulus; (b)  $N_{f50}$  and  $N_{f6}$ ; and (c)  $G_1^*$  and  $G_2^*$ .

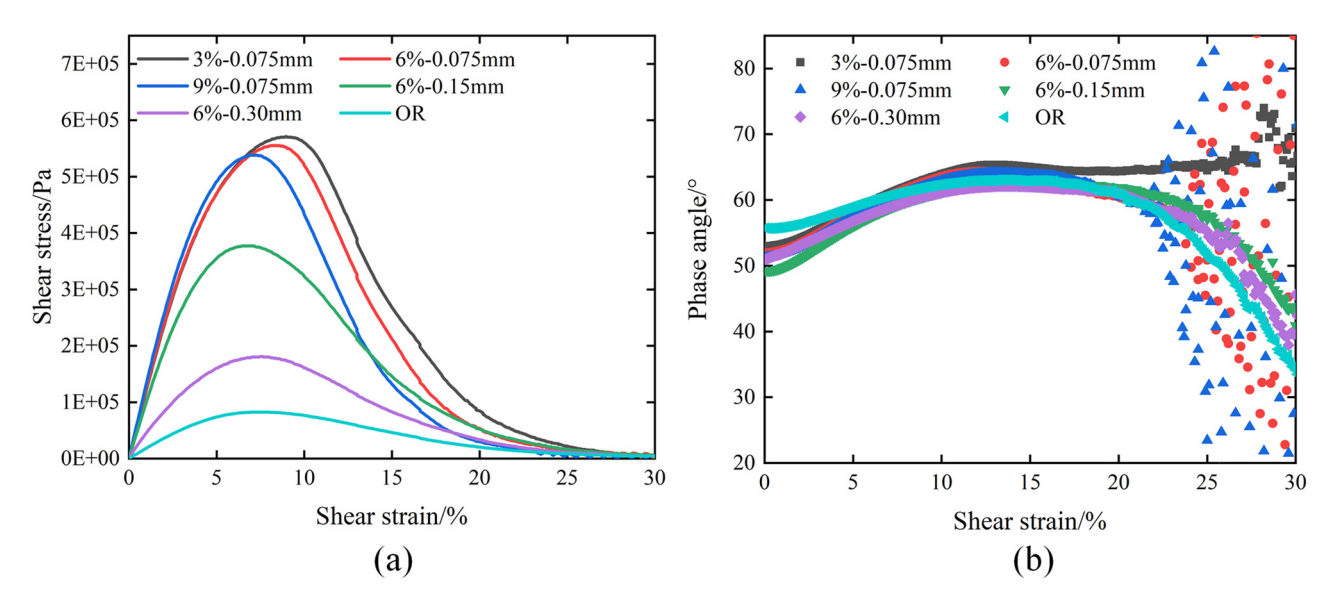


Figure 21: LAS test result of PUA-modified asphalt: (a) stress-strain curve and (b) phase angle-strain curve.

ability of asphalt. Moreover, compared with the particle size of PUA modifier, the dosage of PUA modifier could promote better improving effect on the anti-deformation ability of asphalt.

Based on the testing results of LAS and the calculation method of AASHTO TP-101-12 [39], VECD model, the testing results are shown in Figure 23b, where the ordinate represented the integrity parameter C of asphalt sample, and the abscissa referred to the cumulative damage intensity D. When C was equal to 1, the asphalt was undamaged completely. As the given cumulative damage parameter increased, the integrity of asphalt continued being damaged. When C = 0, the performance of asphalt was failed completely. When the cumulative damage parameter C was given, the larger the D was, the stronger the ability of the material could be to resist damage. According to AASHTO TP-101-12, 35% damage fatigue (C = 0.65) was used as material failure point [39].

From the observation in Figure 23b, it could be seen that under the given cumulative damage parameter *C*, the damage intensity of different PUA-modified asphalts was larger than that of 70# asphalt. Regarding PUA-modified asphalt, the particle size and dosage of PUA would affect the anti-injury ability of asphalt. Therefore, the following section would classify and discuss the effects of particle size and dosage of PUA on the anti-damage property of asphalt.

# 3.4.4.2 Effect of PUA modifier content on mesothermal fatigue performance of asphalt

Figure 24 shows the LAS test results of modified asphalt with different particle sizes of PUA. It could be investigated from Figure 24a that the peak stress of modified asphalts with different particle sizes of PUA was larger than that of 70# asphalt, while with increasing of PUA content, the peak stress of asphalt decreased gradually,

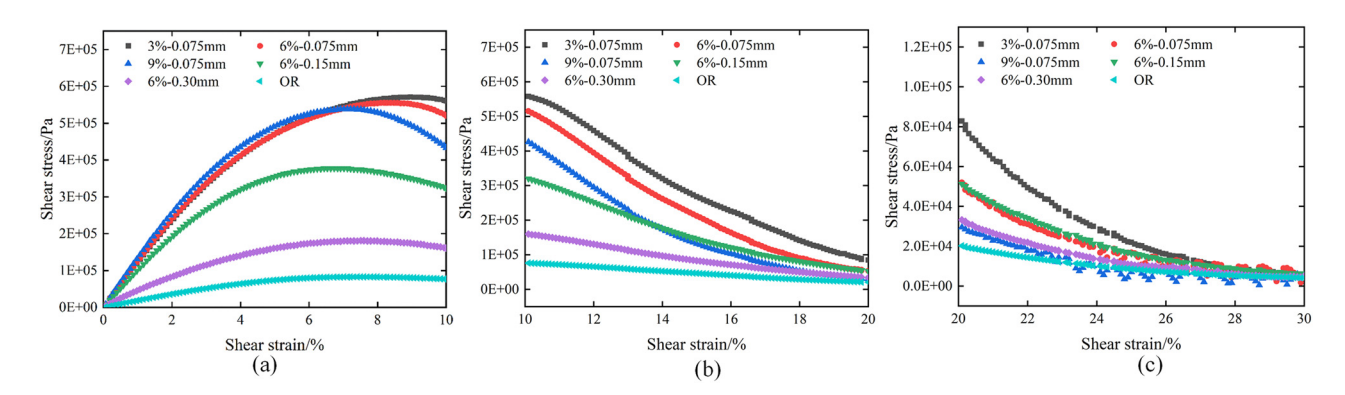


Figure 22: Piecewise diagram of stress-strain curve: (a) 0-10%; (b) 10-20%; and (c) 20-30%.

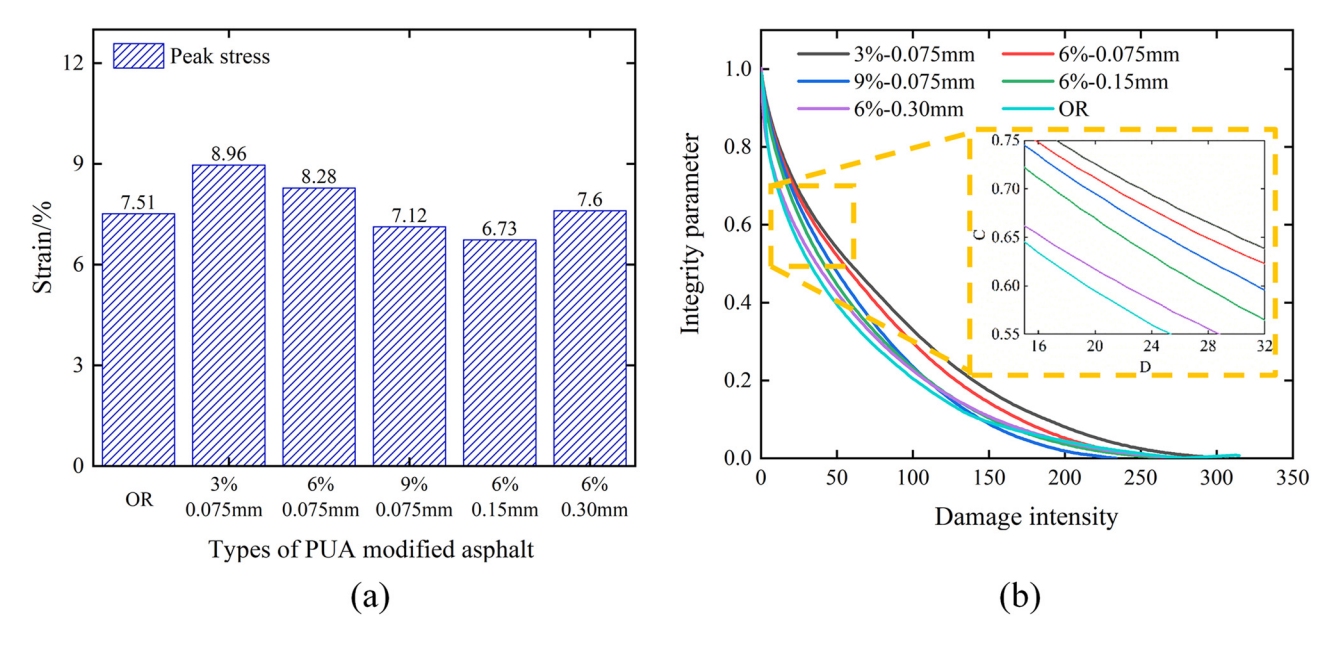


Figure 23: Evaluating indices of LAS test results: (a) Yield strain and strain corresponding to peak phase angle and (b) damage curve.

and the deformation resistance of asphalt decreased gradually. Figure 24a illustrates that the yield strain of PUAmodified asphalt increased from 7.51 to 8.98%, which increased by 19% when dosage rose from 0 to 6%. With the increase in dosage, the yield strain of modified asphalt decreased gradually, and the improving effect of PUA modifier on fatigue resistance of asphalt decreased gradually. When the PUA content reached 9%, the yield strain of modified asphalt decreased by 5% compared with 70# asphalt. According to Figure 24c, when the integrity parameter C = 0.65, the damage intensity D of PUA-modified asphalt was significantly larger than that of 70# asphalt. However, with increasing of PUA content, the damage intensity D of asphalt decreased gradually, and the promoting impact of PUA modifier on the improvement of fatigue resistance of asphalt was weakened.

In summary, the reasonable PUA content could improve the anti-fatigue performance of asphalt effectively, but when the content of PUA continued increasing, enhancing effect on the improvement of fatigue resistance of asphalt could not be well reflected, which might be due to the poor dispersion of high content PUA modifier in asphalt. The PUA modifier could not merge with asphalt, resulting in poor relative stability of the material system, increasing the chance of two-phase separation and weakening the modifying effect [17].

## 3.4.4.3 Effect of PUA modifier particle size on mesothermal fatigue performance of asphalt

Figure 25 presents the LAS test results of modified asphalt with different particle sizes of PUA. From Figure 25a,

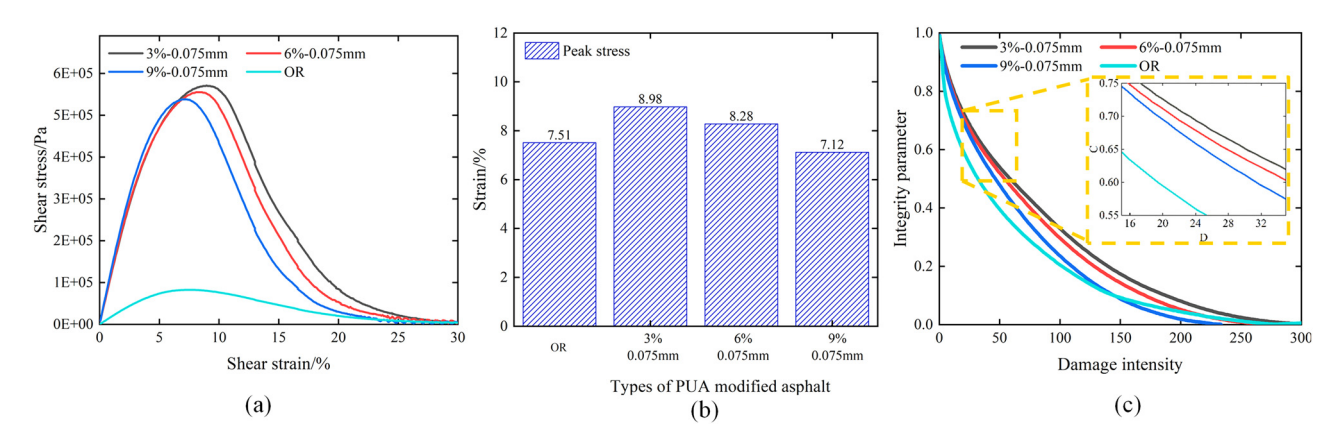


Figure 24: Different contents of PUA: (a) stress-strain curve; (b) peak strain; (c) and damage curve.

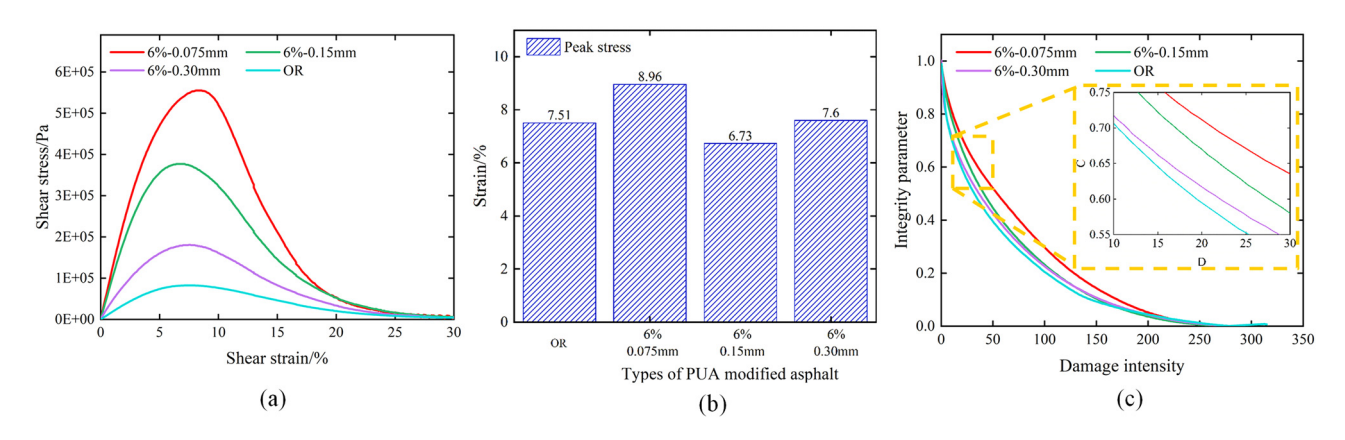


Figure 25: Different particle sizes of PUA: (a) stress-strain curve; (b) peak strain; and (c) damage curve.

performance advantage of PUA-modified asphalt concluded that PUA modifiers of different particle sizes could improve the deformation resistance of asphalt effectively. With the increase in PUA particle size, the peak stress of asphalt decreased gradually. It could be analyzed from Figure 25b that, compared with 70# asphalt, the yield strain of 6% - 0.075 mm PUA-modified asphalt increased by 19%. When particle size rose from 0.075 to 0.15 mm, the yield strain of PUA-modified asphalt increased from 8.96 to 6.73%, which was 10% lower than that of 70# asphalt. When the particle size increased to 0.3 mm, the difference of yield stress between PUA-modified asphalt and 70# asphalt was almost the same. With the particle size of modifier increasing from 0.075 to 0.15 mm, poor compatibility between PUA modifier and asphalt might be the reason resulting in the degradation of modifying effect. However, the yield strain of 6% - 0.3 mm PUAmodified asphalt was higher than that of 6% - 0.15 mm PUA-modified asphalt, and bigger particle of 0.3 mm PUA bore more load instead of asphalt, which led to the higher yield strain than 6% - 0.15 mm PUA-modified asphalt. In the LAS test, most of the internal stress generated by the deformation of asphalt under external force could be effectively absorbed and dispersed by PUA particles, thus showing higher deformation resistance [41].

According to Figure 25c, when C=0.65, the damage intensity D of modified asphalt with different particle sizes of PUA were all larger than those of 70# asphalt. With the decrease in particle size, the damage intensity D and the anti-damage ability of asphalt increased gradually. When the particle size rose to 0.3 mm, the damage intensity D was almost the same as that of 70# asphalt. The smaller the particle size of PUA was, the larger the surface area was and the more uniform the dispersion of PUA in asphalt was, which provided the larger action area integrating with asphalt to promote the formation

of structural asphalt and improving effect on property of asphalt [42–44].

## 4 Conclusions

In this article, the PUA powder modifier was produced through the improved process of 'spraying-preliminary crushing-fine grinding', and the modified asphalt was prepared through applying the different contents and particle sizes of PUA materials. The apparent viscosity of PUA-modified asphalt was analyzed and compared. The MSCR test, the LAS test, and the time sweep test of PUA-modified asphalt were carried out to investigating the impact and effect of PUA on the high temperature creep performance and the improvement of fatigue resistance of asphalt material. The conclusions were detailed as follows:

- A large number of micro spherical structures of different diameters existed in the cross-section of PUA particles. The grinding effect would destroy the integrity of some spherical structures, which might affect the modifying effect on asphalt.
- PUA modifier could improve the viscosity of asphalt significantly and the dosage increase would enhance the improving effect on the apparent viscosity of asphalt.
  Enlarging the particle size would weaken the improving effect of PUA on the viscosity of asphalt.
- The addition of PUA modifier could increase the recovery rate of asphalt and reduce the unrecoverable creep compliance of asphalt effectively, which would improve rutting resistance of asphalt at high temperature. However, the increase in particle size of PUA would degrade the improving effect on asphalt binder.

- Appropriate dosage of PUA could enhance the improving effect of PUA modifier on the anti-fatigue performance of asphalt, but excessive dosage would inhibit its modifying effect. Increasing the particle size of PUA could enhance the anti-deformation performance of asphalt.
- Since the particle size of 0.3 mm PUA modifier was too large to disperse in asphalt effectively, the rheological properties' test was hard to evaluate the actual effect of PUA modifier on asphalt. Thus, the large-size PUA modifier would be used as modifier to be added into the asphalt mixture and the modifying effect would be further discussed.

Funding information: This article describes research activities mainly requested and sponsored by Fundamental Research Funds for the Central Universities (CHD 300102212516), Guangdong Basic and Applied Basic Research Foundation under grant numbers 2019A1515110348 and 2019A1515110397, Special Fund for Science and Technology Innovation Strategy of Guangdong Province under grant numbers pdjh2021a0149 and pdjh2022b0161, Supported by the Fundamental Research Funds for the Central Universities under grant number 300102212516, Guangzhou HuaHui Traffic Technology Co., Ltd. Technical Project under grant number 21HK0242, and Guangdong GuanYue Highway & Bridge Co., Ltd. Enterprise Mission Project under grant number GDKTP2021009700. That sponsorship and interest are gratefully acknowledged.

Author contributions: All authors have accepted responsibility for the entire content of this article and approved its submission.

**Conflict of interest:** The authors state no conflict of interest.

## References

- Wang HP, Guo YX, Wu MY, Xiang K, Sun SR. Review on structural damage rehabilitation and performance assessment of asphalt pavements. Rev Adv Mater Sci. 2021;60(1):438-49.
- Yu H, Yao D, Qian G, Cai J, Gong X, Cheng L. Effect of ultraviolet aging on dynamic mechanical properties of SBS modified asphalt mortar. Constr Build Mater. 2021;281:122328.
- Wang P, Dong ZJ, Tan YQ, Liu ZY. Anti-ageing properties of styrene-butadiene-styrene copolymer-modified asphalt combined with multi-walled carbon nanotubes. Road Mater Pavement Des. 2017;18(3):533-49.
- Liu F, Zheng M, Fan X, Li H, Wang F, Lin X. Properties and mechanism of waterborne epoxy resin-SBR composite modified emulsified asphalt. Constr Build Mater. 2021;274:122059.

- Hermida-Merino D, O'Driscoll B, Hart LR, Harris PJ, Colguhoun HM, Slark AT, et al. Enhancement of microphase ordering and mechanical properties of supramolecular hydrogen-bonded polyurethane networks. Polym Chem. 2018;9(24):3406-14.
- Jin X, Guo N, You Z, Wang L, Wen Y, Tan Y. Rheological properties and micro-characteristics of polyurethane composite modified asphalt. Constr Build Mater. 2020;234:117395.
- Jin X, Guo N, You Z, Tan Y. Design and performance of poly-[7] urethane elastomers composed with different soft segments. Materials. 2020;13(21):4991.
- [8] Bazmara B, Tahersima M, Behravan A. Influence of thermoplastic polyurethane and synthesized polyurethane additive in performance of asphalt pavements. Constr Build Mater. 2018-166-1-11
- Jomaa MH, Roiban L, Dhungana DS, Xiao J, Cavaillé JY, Seveyrat L, et al. Quantitative analysis of grafted CNT dispersion and of their stiffening of polyurethane (PU). Compos Sci Technol. 2019;171:103-10.
- [10] Xu C, Zhang Z, Zhao F, Liu F, Wang J. Improving the performance of RET modified asphalt with the addition of polyurethane prepolymer (PUP). Constr Build Mater. 2019;206:560-75.
- [11] Sun M, Zheng M, Qu G, Yuan K, Bi Y, Wang J. Performance of polyurethane modified asphalt and its mixtures. Constr Build Mater. 2018;191:386-97.
- [12] Peng C, Huang S, You Z, Xu F, You L, Ouyang H, et al. Effect of a lignin-based polyurethane on adhesion properties of asphalt binder during UV aging process. Constr Build Mater. 2020;247:118547.
- [13] Xia L, Cao D, Zhang H, Guo Y. Study on the classical and rheological properties of castor oil-polyurethane pre polymer (C-PU) modified asphalt. Constr Build Mater. 2016;112:949-55.
- [14] Awazhar NA, Khairuddin FH, Rahmad S, Fadzil SM, Omar HA, Yusoff NIM, et al. Engineering and leaching properties of asphalt binders modified with polyurethane and Cecabase additives for warm-mix asphalt application. Constr Build Mater. 2020;238:117699.
- [15] Sun X, Ou Z, Xu Q, Qin X, Guo Y, Lin J, et al. Feasibility analysis of resource application of waste incineration fly ash in asphalt pavement materials. Environ Sci Pollut Res. 2022;30(2):1-16.
- [16] Tian Y, Li H, Sun L, Zhang H, Harvey J, Yang J, et al. Laboratory investigation on rheological, chemical and morphological evolution of high content polymer modified bitumen under long-term thermal oxidative aging. Constr Build Mater. 2021;303:124565.
- Jin X, Sun S, Guo N, Huang S, You Z, Tan Y. Influence on [17] polyurethane synthesis parameters upon the performance of base asphalt. Front Mater. 2021;8:656261.
- Liu M, Han S, Shang W, Qi X, Dong S, Zhang Z. New polyur-[18] ethane modified coating for maintenance of asphalt pavement potholes in winter-rainy condition. Prog Org Coat. 2019;133:368-75.
- [19] Gao W, Bie M, Quan Y, Zhu J, Zhang W. Self-healing, reprocessing and sealing abilities of polysulfide-based polyurethane. Polymer. 2018;151:27-33.
- [20] Cong L, Yang F, Guo G, Ren M, Shi J, Tan L. The use of polyurethane for asphalt pavement engineering applications: A state-of-the-art review. Constr Build Mater. 2019;225:1012-25.

- [21] Zhang Z, Sun J, Jia M, Qi B, Zhang H, Lv W, et al. Study on a thermosetting polyurethane modified asphalt suitable for bridge deck pavements: Formula and properties. Constr Build Mater. 2020;241:118122.
- [22] Xu C, Zhang Z, Zhao F, Liu F, Wang J. Improving the performance of RET modified asphalt with the addition of polyurethane prepolymer (PUP). Constr Build Mater. 2019:206:560-75.
- [23] Xin J, Naisheng G, You Z, Yiqiu T. Research and development trends of polyurethane modified asphalt. Mater Rep. 2019;33(21):3686.
- [24] Sun X, Qin X, Li S, Zou C, Wang C, Wang X. Characterization of thermal insulating micro-surfacing modified by inorganic insulating material. Constr Build Mater. 2018;175:296–306.
- [25] ASTM, D. Standard test method for viscosity determination of asphalt at elevated temperatures using a rotational viscometer. In American Society for Testing and Materials; 2015.
- [26] AASHTO TP 70, T. Standard method of test for multiple stress creep recovery (MSCR) test of asphalt binder using a dynamic shear rheometer (DSR); 2013.
- [27] Sun X, Qin X, Chen Q, Ma Q. Investigation of enhancing effect and mechanism of basalt fiber on toughness of asphalt material. Pet Sci Technol. 2018;36(20):1710-7.
- [28] Sun X, Qin X, Liu Z, Yin Y, Zou C, Jiang S. New preparation method of bitumen samples for UV aging behavior investigation. Constr Build Mater. 2020;233:117278.
- [29] Xin J, Nai-sheng G, Si-meng Y, Tao L, Zhan-ping Y. Preparation and performance evaluation on polyurethane composite modified asphalt. China J Highw Transp. 2021;34(3):80.
- [30] Yang X, Tang H, Cai X, Wu K, Huang W, Zhang Q, et al. Evaluating reclaimed asphalt mixture homogeneity using force chain transferring stress efficiency. Constr Build Mater. 2023;365:130050.
- [31] Wang C, Li Y, Wen P, Zeng W, Wang X. A comprehensive review on mechanical properties of green controlled low strength materials. Constr Build Mater. 2022;2022:129611.
- [32] Liu S, Jin J, Yu H, Gao Y, Du Y, Sun X, et al. Performance enhancement of modified asphalt via coal gangue with microstructure control. Constr Build Mater. 2023;367:130287.
- [33] Jin J, Gao Y, Wu Y, Liu S, Liu R, Wei H, et al. Rheological and adhesion properties of nano-organic palygorskite and linear

- SBS on the composite modified asphalt. Powder Technol. 2021:377:212-21.
- [34] Sun X, Yuan J, Liu Z, Qin X, Yin Y. Evaluation and characterization on the segregation and dispersion of anti-UV aging modifying agent in asphalt binder. Constr Build Mater. 2021;289:123204.
- [35] Yu H, Zhu Z, Leng Z, Wu C, Zhang Z, Wang D, et al. Effect of mixing sequence on asphalt mixtures containing waste tire rubber and warm mix surfactants. J Clean Prod. 2020;246:119008.
- [36] Guo M, Liang M, Sreeram A, Bhasin A, Luo D. Characterisation of rejuvenation of various modified asphalt binders based on simplified chromatographic techniques. Int J Pavement Eng. 2021:1–11.
- [37] Niu D, Xie X, Zhang Z, Niu Y, Yang Z. Influence of binary waste mixtures on road performance of asphalt and asphalt mixture. J Clean Prod. 2021;298:126842.
- [38] Wang S, Wang C, Yuan H, Ji X, Yu G, Jia X. Size effect of piezoelectric energy harvester for road with high efficiency electrical properties. Appl Energy. 2023;330:120379.
- [39] Guo M, Liu X, Jiao Y, Tan Y, Luo D. Rheological characterization of reversibility between aging and rejuvenation of common modified asphalt binders. Constr Build Mater. 2021;301:124077.
- [40] Zhang H, Chen Z, Xu G, Shi C. Evaluation of aging behaviors of asphalt binders through different rheological indices. Fuel. 2018:221:78-88.
- [41] Sun X, Zhang Y, Peng Q, Yuan J, Cang Z, Lv J. Study on adaptability of rheological index of nano-PUA-modified asphalt based on geometric parameters of parallel plate. Nanotechnol Rev. 2021;10(1):1801–11.
- [42] Yu R, Zhu X, Zhou X, Kou Y, Zhang M, Fang C. Rheological properties and storage stability of asphalt modified with nanoscale polyurethane emulsion. Pet Sci Technol. 2018;36(1):85–90.
- [43] Liu F, Zheng W, Li L, Feng W, Ning G. Mechanical and fatigue performance of rubber concrete. Constr Build Mater. 2013;47:711–9.
- [44] Liu F, Chen G, Li L, Guo Y. Study of impact performance of rubber reinforced concrete. Constr Build Mater. 2012;36:604–16.